Structure of planktonic food web in the Gulf of Gabès (Southeastern Mediterranean): potential importance of heterotrophic and mixotrophic microzooplankton

Kaouther Mejri Kousri, Amel Belaaj Zouari, Marouan Meddeb, Oumayma Chkili, Nathalie Niquil, Marc Tedetti, Marc Pagano, Cherif Sammari, Yosra Khammeri, Malika Bel Hassen, et al.

Aquatic Sciences (2023) 85:61
https://doi.org/10.1007/s00027-023-00954-y

Aquatic Sciences

RESEARCH ARTICLE

Structure of planktonic food web in the Gulf of Gabès (Southeastern Mediterranean): potential importance of heterotrophic and mixotrophic microzooplankton

Kaouther Mejri Kousri[1,2] · Amel Belaaj Zouari[2] · Marouan Meddeb[1,3] · Oumayma Chkili[1,3,4] · Nathalie Niquil[4] · Marc Tedetti[5] · Marc Pagano[5] · Cherif Sammari[2] · Yosra Khammeri[2] · Malika Bel Hassen[2] · Asma Sakka Hlaili[1,3]

Received: 24 June 2022 / Accepted: 8 March 2023

Abstract

The planktonic food web structure was investigated in a productive Mediterranean gulf during spring and fall. Plankton communities, rates of primary production (PP), bacterial production (BP) and grazing by microzooplankton and mesozooplankton were examined in a station influenced by Saharan dust, St1; a station located in the Boughrara Lagoon, St2; and a polluted station, St3, close to a phosphate industrial site. The high nutrient (12–17 µM) and chlorophyll *a* (Chl *a*) concentrations (3.7–16.9 mg m^{-3}) as well as the high rates of PP (1123–2638 mg C m^{-2} d^{-1}) and BP (128–1337 mg C m^{-2} d^{-1}), recorded throughout the sampling period, indicated the eutrophic character of the study site. Microzooplankton and mesozooplankton mostly showed seasonal changes in their composition and grazing rates. During spring, PP was dominated by nano- and micro-sized fractions, but pico-, nano- and microphytoplankton contributed equally to Chl *a*. Heterotrophic and mixotrophic microzooplankton consumed significant proportions of the daily production for bacterioplankton (50–72%) and size-fractioned phytoplankton (25–86%), whereas herbivorous copepods grazed daily on 13–15% of PP. These trophic links suggested that the multivorous food web prevailed in spring. During fall, picophytoplankton, mainly *Synechococcus*, dominated the Chl *a* and PP in St1, where microbivorous microzooplankton (mainly mixotrophic dinoflagellates) grazed ≥ 50% of the production of bacterioplankton and picophytoplankton, while mesozooplankton, dominated by detritivorous copepods, removed only 5% of PP, suggesting a microbial food web. In St2 and St3, Chl *a* and PP were dominated by large phytoplankton, which was substantially grazed by heterotrophic and mixotrophic microzooplankton (42–62% grazed d^{-1}) and copepods (12–25% grazed d^{-1}), indicating a carbon channeling throughout the herbivorous food web. The seasonal and spatial change in the planktonic food web implies different efficiencies in the export of carbon. Even in productive waters, picophytoplankton along with microzooplankton, including mixotrophic and heterotrophic organisms, significantly contribute to the ecological functioning of these systems and play a central role in structuring the carbon transfer pathway.

Keywords Mixotrophic and heterotrophic microzooplankton · Zooplankton grazing · Planktonic food web · Southeastern Mediterranean

✉ Asma Sakka Hlaili
asma.sakkahlaili@gmail.com

[1] Faculté des Sciences de Bizerte, Laboratoire de Biologie Végétale et Phytoplanctonologie, Université de Carthage, Bizerte, Tunisia

[2] Present Address: Institut National des Sciences et Technologies de la Mer (INSTM), 28, rue 2 mars 1934, 2025 Salammbô, Tunisia

[3] Faculté des Sciences de Tunis, Laboratoire des Sciences de l'environnement, Biologie et Physiologie des Organismes Aquatiques LR18ES41, Université de Tunis El Manar, Tunis, Tunisia

[4] CNRS, Normandie Université, UNICAEN, UMR BOREA (MNHN, CNRS-8067, Sorbonne Université, Université Caen Normandie, IRD-207, Université des Antilles), 14032 Caen, France

[5] Aix-Marseille University, Université de Toulon, CNRS, IRD, MIO UM 110, Marseille, France

Published online: 01 April 2023

Introduction

The planktonic food web (PFW) deeply influences the flow of matter and energy in marine biota. The determination of the structure of PFW is central to understanding the functioning of marine ecosystems and to predictig their responses to diverse environmental and anthropogenic changes (Thompson et al. 2012; Meddeb et al. 2019). For the last 3 decades, two main concepts of PFW have been reported with evolutions for each of them. The linear food chain, assigned later as the herbivorous food web, and the bacterial loop were the earliest to be recognised (Rhyter 1969; Azam et al. 1983). As trophic interactions within the planktonic community were found to be more complex, the multivorous food web and microbial food web, including polymicrobial and phytomicrobial pathways, were then proposed (Legendre and Rassoulzadegan 1995; Sakka Hlaili et al. 2014). In fact, the size and composition of producers and grazers determine the magnitude of primary production and carbon transfer throughout the food web. It has been acknowledged that herbivorous and multivorous food webs, in which mesozoplankton (i.e. copepods) graze significantly on large phytoplankton (i.e. diatoms), can channel a large amount of carbon to higher consumers and, hence, dominate in high productive ecosystems (Cushing 1989; Calbet et al. 2016). In less productive waters, the microbial loop and microbial food web, dominated by microzooplankton grazing on bacteria and small phytoplankton, are less efficient in carbon channeling, since most carbon can be lost and remineralised (Legendre and Gosselin 1989; Legendre and LeFèvre 1989). This perception has been modified since there is increasing evidence that microzooplankton can also play a substantial role in channelling carbon in high productive waters, where microbial food webs can be dominant (Vargas et al. 2007; Grami et al. 2008). Indeed, microzooplankton, which are often dominated by protozoan organisms such as heterotrophic ciliates and dinoflagellates, are abundant in coastal waters (Sakka Hlaili et al. 2007; Sherr et al. 2009), where they can consume > 60% of phytoplankton production (Calbet and Landry 2004; Buitenhuis et al. 2010; López-Abbate 2021). Large heterotrophic dinoflagellates and ciliates could have greater grazing impact on large phytoplankton than copepods (Jeong et al. 2004; Sakka Hlaili et al. 2007; Meddeb et al. 2018). Furthermore, several protozoans, particularly dinoflagellates, which have been thought to be exclusively autotrophic, have been revealed as mixotrophic, leading in the past to potential underestimation of their grazing (Calbet 2008). These mixotrophs have different feeding mechanisms and are able to feed on diverse types of prey, including bacteria, picophytoplankton, nanoflagellates and diatoms (Jeong et al. 2005, 2010; Seong et al. 2006). Therefore, the role of microzooplankton in the different types of PFW may be more complex than previously thought, especially in ecosystems where mixotrophic organisms are abundant.

Different types of PFW have been reported in the Mediterranean Sea. The microbial food web and microbial loop were documented in oligotrophic open sea areas, where small producers and nanoheterotrophs are generally dominant (such as the Aegean, Ionian, Adriatic, Ligurian and Levantine Seas) (Šolić et al. 2010; Christaki et al. 2011; Tanaka et al. 2003, 2011; Giannakourou et al. 2014; Pulido-Villena et al. 2014; Livanou et al. 2019). Conversely, coastal Mediterranean ecosystems support high-nutrient waters and host large algal development and intense diatom-bloom occurrence (Davidson et al. 2012; Carstensen et al. 2015). Copepods seasonally dominate the mesozooplankton (Hannides et al. 2015; Zakaria et al. 2018); then, primary production can efficiently be transferred to higher consumers throughout herbivorous food webs (Alekseenko et al. 2014; Calbet et al. 2016). The studies on PFW in the Mediterranean have mainly been conducted in the Northern part and, to a small extent, in the southern part (Grami et al. 2008; Sakka Hlaili et al. 2008; Meddeb et al. 2018, 2019). This North-South imbalance could limit the inter-system comparison and the understanding of the ecosystem functioning of the Mediterranean Sea. The Gulf of Gabès (hereafter referred to as the Gulf), including the Lagoon of Boughrara, is considered one of the most productive areas of the Mediterranean Sea (D'Ortenzio and d'Alcalà 2009; Béjaoui et al. 2019). However, it is still unclear how carbon is channeled to higher consumers within the Gulf ecosystem. In the latter, heterotrophic and mixotrophic protozoans, including dinoflagellates, nanoflagellates and ciliates, can reach high concentrations up to maximum of 10^9 cells L^{-1}, suggesting their strong top-down control on phytoplankton (Drira et al. 2008, 2009; Hamdi et al. 2015; Feki-Sahnoun et al. 2017, 2020). High abundance of the mesozooplankton, mostly dominated by herbivorous copepods, was also reported in this area (Hannachi et al. 2008; Drira et al. 2009, 2017; Makhlouf Belkahia et al. 2021). The previous studies in the Gulf suggest the dominance of the multivorous food web, where microbial and herbivorous pathways both would play important roles in channeling carbon. Furthermore, trophic functioning within the Gulf should change, since the plankton communities showed significant seasonal and spatial dynamics related to the change of environmental conditions (Bel Hassen et al. 2008, 2009; Drira et al. 2009; Makhlouf Belkahia et al. 2021). Seasonal variation on PFW has already been reported in other coastal regions such as the Bay and the Channel of Bizerte (SW Mediterranean), where Meddeb et al. (2019) found an herbivorous food

web in spring and summer and multivorous and microbial food webs in autumn and winter. Shifts in PFW structure and functioning among seasons were also observed in coastal systems (Northeast US Shelf and Southeast Japan) and were related to the seasonal variations of environmental conditions and phytoplankton size composition (Shinada et al. 2005; Marrec et al. 2021).

The present study is an investigation of carbon trophic transfer in highly productive Southeastern Mediterranean waters, by considering all planktonic components from bacterioplankton to mesozooplankton. The main goal is to depict the structure of PFW during two different seasons and to assess the importance of different microbial communities in channeling biogenic carbon. The results will provide new insights into the functional roles of heterotrophic and mixotrophic microzooplankton and contribute to a better understanding of the pelagic system functioning in the Southern Mediterranean region. This will support future ecological modelling of the structural and functional characteristics of the PFW and its response to environmental change pressure.

Materials and methods

Study area

The Gulf of Gabès is an area wide in length and width that is bound by Djerba Island to the Southeast and the Kerkennah Islands to the Northeast (Fig. 1a). It is one of the largest continental shelves in the Eastern Mediterranean characterised by one of the highest tide amplitudes (up to 2 m). The hydrodynamics of the Gulf are driven by local forcing, including tidal currents, wind-induced drift currents, onshore-offshore baroclinic currents and the southern branch of the Modified Atlantic Water (MAW) (Othmani et al. 2017; Boukthir et al. 2019). The Gulf is also characterised by high nutrient availability, resulting from anthropogenic loadings, sediment resuspension events and inputs of Saharan dust (Bel Hassen et al. 2009; Drira et al. 2009; Khammeri et al. 2018). Phosphorous nutrients are particularly high (> 3 µM for PO_4^{3-}, > 10 µM for organic P; El Kateb et al. 2018) because of the development of the phosphate industry (since 1972) and the discharge of phosphogypsum (~ 12,000 ton per day), which also bring several metallic pollutants into the Gulf

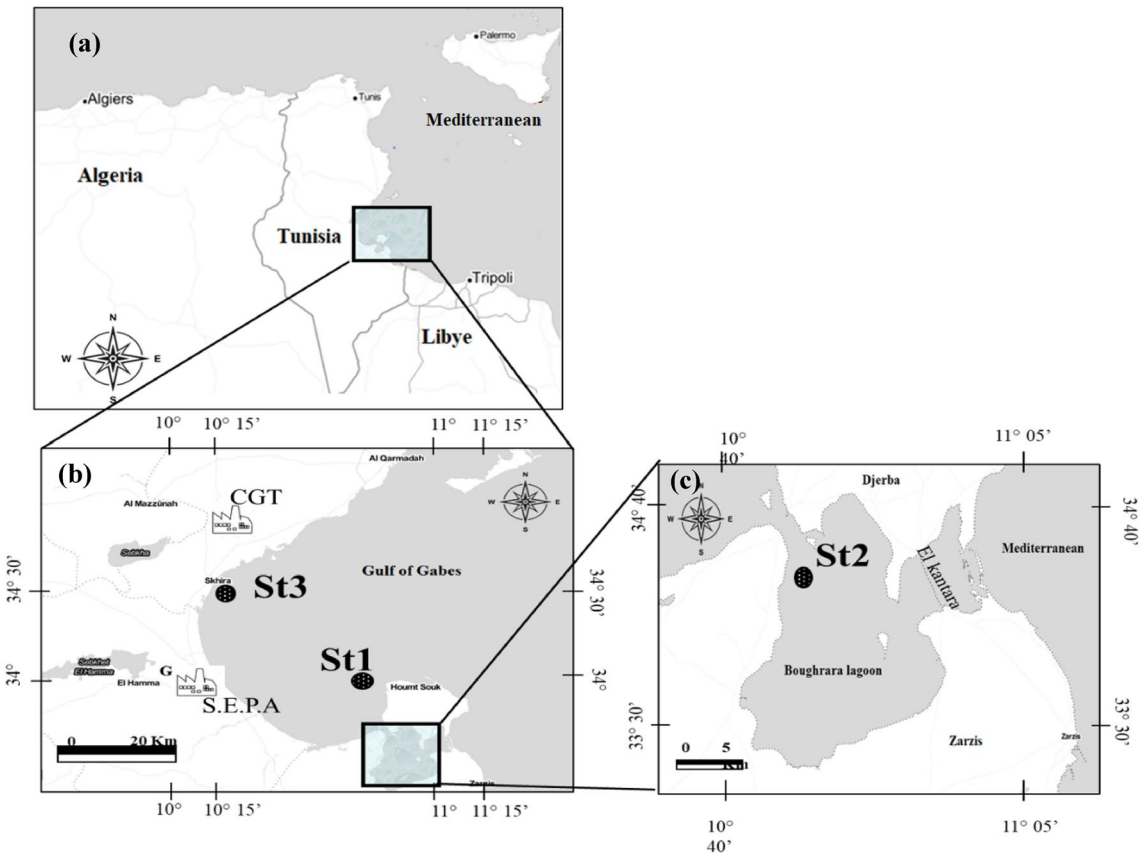

Fig. 1 Location of the three study stations in Gulf of Gabès (Southeastern Mediterranean Sea, Tunisia)

(Khedhri et al. 2014; Boudaya et al. 2019; Kmiha Megdiche et al. 2019).

The Lagoon of Boughrara (Fig. 1a) is a semi-closed ecosystem located at the Southwestern part of the Gulf that supports aquaculture and fishing. It is a shallow lagoon (< 10 m depth and 500 km^2 surface area) characterised by a very high net evaporation, leading to higher salinity (> 40) than in surrounding sites (Feki-Sahnoun et al. 2014). The poor water exchange between the Lagoon and the Mediterranean Sea has enhanced the eutrophisation of the Lagoon in recent decades (Feki-Sahnoun et al. 2017). The Lagoon is also affected by the phosphogypsum discharge, reflecting in loadings of phosphorus, organic matter and heavy metals (Khedhri et al. 2014).

Sampling

Sampling was conducted during April (herein referred to as spring) and November 2017 (herein referred to as fall) at three stations (Fig. 1) with specific environmental features. Station St1 (33° 52′ 54″ N, 10° 42″11″ E, 12 m maximal depth, Fig. 1b), located in the marine coastal area of Jerba Island, is subject to nutrient supply by Saharan dust (Hamza et al. 2016). Station St2 (33° 39′ 14″ N, 10°46′14″ E, 8 m maximal depth, Fig. 1c), located in the Lagoon of Boughrara, is considered a very eutrophic site (Feki-Sahnoun et al. 2017). Station St3 (34° 24′ 58″ N, 10° 21′40″ E, 7 m maximal depth, Fig. 1b) is situated on the coast of Skhira city, where the main phosphate industrial site was installed. For each station, water was collected using a 5-l plastic water sampler (Hydro-Bios), at three depths (2, 4 and 8 m for St1; 2, 4 and 6 m for St2; 0.5, 2.5 and 4 m for St3). Seawater samples were filtered through a 200-µm mesh screen (to remove debris and large zooplankton) and then stored in polyethylene containers for further chemical and biological analyses. Then, temperature, salinity, pH and dissolved oxygen were measured on the raw seawater samples using a multi-probe sensor (Multi 1970i, WTW). Mesozooplankton samples were collected using a WP2 200-µm mesh net with a ring diameter of 28 cm. The net was towed vertically at a speed of 1 m s^{-1} from depths of 10 m at St1, 9 m at St2 and 6 m at St3 to the surface. A flow meter was used to determine the water volume filtered during the net tow.

Nutrients, POC and Chl *a* analyses

Nutrient subsamples (100 ml) were immediately stored at − 20 °C and in the dark until the analysis. Nutrients were analysed using an autoanalyser type 3 (Bran and Luebbe). The detection limits were 0.004 mg dm^{-3} for NO_2^-, 0.009 mg dm^{-3} for NO_3^-, 0.007 mg dm^{-3} for NH_4^+, 0.018 mg dm^{-3} for PO_4^{3-} and 0.012 mg dm^{-3} for $Si(OH)_4$.

For POC analysis, seawater samples were filtered onto pre-combusted (450 °C overnight) 25-mm Whatman GF/F filters (0.7 µm pore size). After filtration, the filters were placed in glass tubes and immediately frozen. In the laboratory, they were dried at 60 °C for 24 h and stored in glass tubes until analysis was performed. Before analysis, filters were acidified with H_2SO_4 to remove inorganic carbon. POC was determined by high temperature combustion (900 °C) and was performed with a CN Integra mass spectrometer, according to Raimbault et al. (2008).

For Chl *a* analysis, subsamples of 1000 ml were successively filtered through 10-, 2- and 0.2-µm pore-size polycarbonate filters to obtain Chl *a* in three size classes of phytoplankton (> 10 µm, 2–10 µm and < 2 µm). The pigments on the filters were then extracted in 90% acetone at 4 °C and stored in the dark overnight, and Chl *a* concentrations were determined using the spectrophotometric method, following the procedure given by Parsons et al. (1984).

Plankton analyses and carbon biomass estimation

Abundances of small phytoplankton and bacterioplankton were determined through flow cytometry analyses, according to Khammeri et al. (2018, 2020). Seawater subsamples (1.8 ml) were immediately fixed with 0.2 ml of a 20% (w/v) paraformaldehyde solution, pH 7.2, incubated at 4 °C in the dark for 20 min, frozen in liquid nitrogen on board and then stored at -80 °C in the laboratory. Fixed samples were analysed with a CyFlow® Space flow cytometer (Sysmex Partec) equipped with a blue diode-pumped solid-state laser (20 mW) at a wavelength of 488 nm and a red diode laser at a wavelength of 638 nm (25 mW). Phytoplankton groups (picoprokaryotes, picoeukaryotes and nanoeukaryotes) were resolved based on their red (FL3, 675 ± 25 nm) and orange (FL2, 590 ± 25 nm) autofluorescence signals, corresponding to the presence of Chl *a* and phycoerythrin pigments (Fig. S1). The forward light scatter (FSC) and the side light scatter (SSC) were used to characterise the cell size, structure and shape. Bacterioplankton were stained with SYBR Green-I (Invitrogen) and incubated in the dark for 15 min before acquisition triggered the green fluorescence signal (FL1, 536 ± 30 nm). Bacteria were distinguished based on their green fluorescence and side light scatter (SSC) signals. The flow cytometric analysis revealed five phytoplankton and one bacterial groups (Fig. S1). Nanoeukaryotes (R1) were characterised by the highest red fluorescence and *Synechococcus* (R4) by the highest orange fluorescence signals. Picoeukaryotes (R2) had low red and orange signatures. Two groups of nano-sized eukaryotes were detected and were labelled as Nano1 MFLR (R3) and Nano2 HFLO (R5) (Khammeri et al. 2020). The Nano1 MFLR and Nano2 HFLO cells had similar red and orange fluorescence signals to the picoeukaryotes and *Synechococcus* groups, respectively, but higher FSC and

SSC signatures, comparable to those of the nanoeukaryotes group, R1. These groups were previously observed in the Gulf (Khammeri et al. 2020). Bacterioplankton (R7) tended to show marked distributions of FL1 (green fluorescence) versus the SSC plot.

Samples for identification and counting of large phytoplankton were fixed in a 3% acid Lugol solution and microzooplankton were fixed in a 4% alkaline Lugol solution (Parsons et al. 1984; Sherr and Sherr 1993). Abundances were determined under an inverted microscope (Motic AE31E, 100× objectives) in 100 ml settled volumes (Utermöhl 1931). At least 500 phytoplankton cells and 200 microzooplankton cells were counted in each sample. During our study, microzooplankton included heterotrophic ciliates (identified as aloricates and tintinnids), heterotrophic nanoflagellates and mixotrophic ebridian flagellates (Hargraves 2002; Jafari et al. 2015). Dinoflagellates were considered to be within the micrograzer's community, as most of them are phagotrophic (Stoecker 1999; Sakka Hlaili et al. 2007). Dinoflagellates were identified as heterotrophic (HDino) or mixotrophic (MDino) organisms, according to the literature (Jacobson and Anderson 1996; Jeong et al. 2010; Boutrup et al. 2016). Other metazoan microzooplankton, such as copepods nauplii and sarcodines, were extremely scarce in our samples and were therefore excluded from the micrograzer's community.

Samples for mesozooplankton analysis were immediately fixed after sampling with borate-buffered formalin (5% final concentration). A count of metazoans was performed under a Leica M205C stereo microscope. All organisms were identified to the lowest possible taxonomic level, according to Trégouboff and Rose (1957) and Razouls et al. (2005, 2020).

For different planktonic groups (from bacteria to microzooplankton), the biovolume of each taxon was determined after measuring its dimensions and applying a standard geometric formula to it. The carbon biomass of each group was then determined by multiplying the carbon content of different taxa by their abundances as detailed in Meddeb et al. (2018). For each planktonic group, carbon biomass (mg C m^{-3}) from the three sampled depths were used to calculate the integrated carbon biomasses expressed in mg C m^{-2}.

Dilution experiments

Dilutions experiments (Landry and Hassett 1982) were carried out at the three study stations, at the same time as sampling, to estimate growth rates of bacterioplankton and of each phytoplankton size fraction as well as their grazing rates by microzooplankton. The dilution technique is a simple standard method that has been used for the last few decades in various ecosystems from open sea to the coastal zone (Landry and Calbet 2004; Pecqueur et al. 2022) since it simultaneously provides growth and grazing rates. This technique was performed also to measure primary production since it gives production rates that are reasonable proxies for ^{14}C estimated production (Brown et al. 2002; Dokulil and Qian 2021). Seawater was collected at the depth of Chl *a* maximum (4 m for St1; 2 m for St2; 2.5 m for St 3), which was determined before sampling, then filtered through a 200-µm mesh screen. The < 200 µm prescreened water served to prepare dilution levels at 25, 50, 75 and 100%, using particle-free seawater obtained by filtration on a 0.2 µm sterile capsule filter (75 Polycap, AS). Each dilution mixture was distributed into three clean 2-l polycarbonate bottles, and dilution bottles were incubated in situ for 24 h. Samples were taken from all dilution levels, before and after incubation, to analyse the different plankton groups (bacterioplankton, size-fractioned phytoplankton and microzooplankton) as described above.

Based on the exponential model of growth, the apparent growth rate (r, d^{-1}) of size-fractioned phytoplankton or bacterioplankton, from each dilution level, was calculated according to the formula

$$r = \ln \frac{C_t}{C_0} \times \frac{1}{t}$$

where C_0 and C_t are the initial and final carbon biomass, respectively, and t is the incubation duration (1 day). The linear regression of r against the dilution level was derived in order to obtain the specific growth rate (k, d^{-1}) of phytoplankton or bacterioplankton (y-axis intercept) and their grazing rate (g, d^{-1}, regression slope) (Landry and Hassett 1982; Landry et al. 2003). The significance of the regression slope was statistically verified (Student's t test, $p < 0.05$) for all types of prey and in all dilution experiments.

To avoid possible artefacts on grazing estimates, the net growth rate of microzooplankton was estimated (Sakka Hlaili et al. 2007) as:

$$R\left(d^{-1}\right) = \ln \frac{Z_t}{Z_0} \times \frac{1}{t}$$

where Z_0 and Z_t are the initial and final (after 1 day) biomass of protozoans, respectively, in undiluted bottles (100%). Then, the corrected grazing rate (g_{corr}, d^{-1}) was calculated (Gallegos 1989) as: $g_{corr} = \frac{\frac{C_t}{C_0} - e^{(kt)} \times (R-k)}{e(Rt) - e(kt)}$

For each prey, coefficients g and g_{corr} were not significantly different (t test, $p > 0.05$), indicating a non-saturated grazer feeding response during our experiments. Therefore, coefficient g was used for further calculations. Production rates (P) of bacterioplankton and size-fractionated phytoplankton and their consumption rates by microzooplankton (G) were calculated according to several authors (Sakka Hlaili et al. 2007; Grattepanche et al. 2011; Meddeb et al. 2018) as:

$$P\left(\text{mg C m}^{-3}\text{d}^{-1}\right) = C_{\text{m}} \times k$$

$$G\left(\text{mg C m}^{-3}\text{d}^{-1}\right) = C_{\text{m}} \times g$$

where C_{m} is the average biomass of bacterioplankton or phytoplankton for 1 day and was calculated as: $C_{\text{m}} = \frac{C_{\text{i}} \times [e^{(k-g)t}]}{(k-g) \times t}$ where C_{i} (mg C m^{-3}) is the initial biomass of bacterioplankton or phytoplankton. Then, the rates P and G were multiplied by the depth of the station to get the depth-integrated rates (mg m^{-2} d^{-1}). The depth-integrated production rates for the three size fractions were added to get the total phytoplankton production.

The percentage of the bacterial or phytoplankton production consumed by microzooplankton was calculated as: $\%P \text{ grazed } \left(d^{-1}\right) = 100 \times \frac{G}{P}$.

Mesozooplankton gut content analysis

The grazing impact of mesozooplankton was measured by the gut fluorescence method, which has been widely used to assess the consumption of phytoplankton by metazooplancton, such as copepods (Irigoien 1998; Tseng et al. 2008; Meddeb et al. 2018). Mesozooplankton samples were collected at each station and during each season, as described above. The net was rinsed, and the cod end content was immediately narcotised with 10% carbonated water (final concentration, v/v) to minimise stress and gut evacuation of the zooplankton (Kleppel and Pieper 1984). Three subsamples (500 ml) were taken from the cod and were kept frozen in the dark to minimise faecal pellet production by the organisms (Saiz et al. 1992). Subsamples were filtered onto 47-mm-diameter GF/F filters, wrapped in foil, immediately frozen and stored in liquid nitrogen until the pigment extraction. These filters were homogenised in 90% acetone, using a motorised tissue homogeniser, and filtered through 25-mm GF/F filters to remove any pulp. The extracted gut pigment was measured before and after acidification with 10% hydrochloric acid, using the spectrophotometric method (Parsons et al. 1984).

The gut pigment content (GP) was calculated, according to Slaughter et al. (2006) as:

$$\text{GP}\left(\text{mg pigment m}^{-3}\right) = \frac{C_{\text{sub}} \times v}{F \times V1}$$

where C_{sub} (mg pigment m^{-3}) is the phaeopigment concentration in the subsample, v (m^3) is the volume of the subsample, F is the fraction of the subsample processed for gut pigment content, and V1 (m^3) is the total volume of water filtered during the net tow. The consumption rate of phytoplankton by mesozooplankton was calculated as:

$$G'\left(\text{mg } C \text{ m}^{-2} \text{ d}^{-1}\right) = D \times \left[\text{GP} \times \text{CR} \times \frac{C}{\text{Chl}a}\right]$$

where D (m) is the depth of the net tow; C:Chl a is the depth-averaged C:Chl a ratio determined for > 2 µm phytoplankton at each station and season, and CR (d^{-1}) is the gut clearance rate of the mesozooplankton. This rate, which is temperature dependent, was determined based on the gut clearance rate constant [K min^{-1} = 0.0117 + (0.001794 × temperature)] given by Dam and Peterson (1988). The percentages of the phytoplankton production consumed by mesozooplankton was calculated as:

$$\%P \text{ grazed } \left(d^{-1}\right) = \frac{G'}{P} \times 100$$

The percentage of standing crop consumed by mesozooplankton was calculated as:

$$\%\text{ Chl } a \text{ grazed } \left(d^{-1}\right) = \text{GP} \times \frac{\text{CR}}{C_{\text{D}}} \times 100$$

where P is the production rate of > 2 µm phytoplankton (estimated by the dilution method), and C_{D} is the depth-average of > 2 µm Chl a at each station and during each season.

Calculation of field unmeasured rates

The rate of microzooplankton production was obtained by multiplying their total consumed carbon (i.e. the sum of consumption rates on bacterioplankton and size-fractioned phytoplankton) by the lower (25%) and the upper limit (50%) of zooplankton growth efficiency (Vézina and Pahlow 2003). The production of micrograzers was considered as the mesozooplankton predation on microzooplankton (G'z). Then, the sum of the consumption rates of mesozooplankton on phytoplankton (i.e. the rate G' estimated by the gut content analysis) and on microzooplankton (i.e. the rate G'z) allowed us to estimate the rate of total carbon consumed by mesozooplankton (i.e. herbivory and carnivory). Finally, this total consumption rate of mesozooplankton was multiplied by the lower (25%) and upper limit (50%) of zooplankton growth efficiency (Vézina and Pahlow 2003) to get the production rate of metazoans, which was assumed to be the carbon potentially available for higher consumers.

The production rate of nano- and microphytoplankton minus their consumption rates by microzoooplankton (i.e. rate G) and mesozooplankton (i.e. rate G') gives the rate of carbon that would potentially sink (i.e. sedimentation).

Statistical analyses

The spatial and seasonal variations on plankton estimates (biomasses, abundances and rates of growth, grazing, production and consumption) were tested by an analysis of

variance (ANOVA). The assumption of normality of data distribution (Kolmogorov-Smirnov test) and homogeneity of variance (Bartlett-Box test) were respected. Spearman correlation (r_s) was used to test different relationships between preys, grazers and environmental factors. ANOVA and correlation analysis were performed in SPSS software18.0 for Windows.

A principal component analysis (PCA) was applied on environmental variables to assess the similarities and differences among stations and seasons and the relevant factors responsible for the differentiation. The R library *Rcmdr* was used with the plugin FactoMineR version 2.7-1 (Lê et al. 2008). The PCA was based on data centered and scaled to unit variance.

To reveal the co-structure between the prey and their potential grazers, a *co-inertia* analysis was applied (Chessel and Mercier 1993; Dolédec and Chessel 1994). This multivariate analysis is a symmetric coupling method, providing a decomposition of the *co-inertia* criterion on a set of orthogonal vectors, defining independent axes of maximum covariance (Chessel and Hanafi 1996). In our study, the two tables used were: (1) the consumption rates of preys by microzooplanton per station and season and (2) the biomass of microzooplankton per station and season. Applying this method aims at linking the grazing rates on the prey and the biomass of their potential consumers. The *co-inertia* was carried out with the *coinertia* function of the ADE4 package with R 4.1.2, after carrying out a standardised PCA on each of the two tables (7 grazing rates and 5 biomasses of grazers for 6 stations/seasons). A between-class analysis (BCA, Dolédec and Chessel 1987; Culhane et al. 2002) was then performed on the two standardised PCAs. Spearman correlations were related to this analysis and were also used with R 4.1.2 to investigate the relationships between the consumption of prey and biomass of micrograzers.

Results

Environmental factors

The first two components of the PCA on environmental variables explain 73% of the total variance showed a clear distinction between seasons and stations (Fig. 2). The seasons were mainly distinguished through the vertical axis, which was positively correlated with PO_4^{3-} ($r=0.6$, $p<0.05$, $N=18$) and $Si(OH)_4$ ($r=0.7$, $p<0.01$, $N=18$) and negatively correlated with total nitrogen ($N=NO_2^- + NO_3^- + NH_4^+$) ($r=-0.7$, $p<0.01$, $N=18$) and Chl *a* ($r=-0.8$, $p<0.01$, $N=18$). The horizontal axis, which was positively correlated with POC ($r=0.5$, $p<0.01$, $N=18$) and temperature ($r=0.9$, $p<0.01$, $N=18$) and negatively with salinity ($r=-0.9$, $p<0.01$, $N=18$), allowed the discrimination of the three stations during each season. Concerning the seasonal variation, the PO_4^{3-} and $Si(OH)_4$ concentrations recorded in spring were higher than in fall. Conversely, the N concentrations measured in spring were lower than those found in fall (Table 1, ANOVA, $p<0.05$, $N=18$). Temperature was higher in spring than fall (Table 1, ANOVA, $p<0.05$, $N=18$), while salinity, pH, dissolved oxygen and POC varied little between seasons (Table 1, ANOVA, $p>0.05$, $N=18$). Lower Chl *a* concentrations were measured in spring (3.31–4.73 mg m^{-3}) compared to fall (4.91–16.86 mg m^{-3}) (Table 1, ANOVA, $p<0.05$, $N=18$). Regarding the spatial

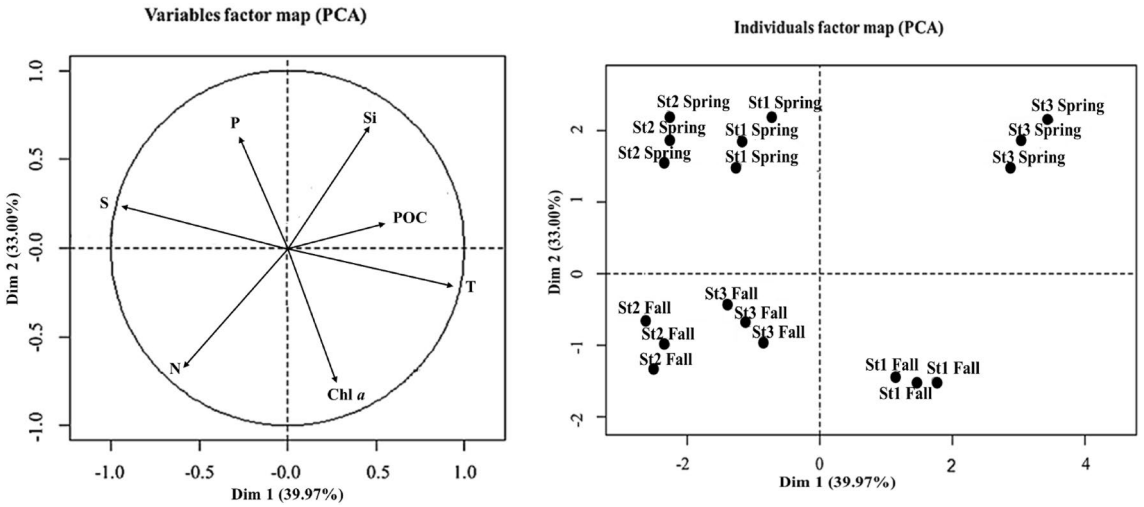

Fig. 2 Principal component analysis (PCA) conducted on the mean values of the main environmental parameters for the three stations during the spring and fall 2017. On the left: variable correlation circle; on the right: distribution of samples through the two axis. *S* salinity, *T* temperature, *N* concentration of $NO_2^- + NO_3^- + NH_4^+$, *P* concentration of PO_4^{3-}, *Si* concentration of $SiOH_4$, *POC* concentration of particulate organic carbon

Table 1 Depth average environmental factors and Chl *a* concentrations and depth integrated carbon biomasses in the study stations during the spring and fall 2017 (mean values ± SD, $N = 18$)

	Spring			Fall		
	St1	St2	St3	St1	St2	St3
Temperature (°C)	17.78 ± 0.26	17.80 ± 0.15	23.95 ± 0.07	16.58 ± 0.67	15.00 ± 1.27	15.40 ± 0.14
Salinity	38.55 ± 0.01	42.57 ± 0.23	39.15 ± 0.07	39.20 ± 0.14	42.35 ± 0.07	40.10 ± 0.42
pH	8.17 ± 0.12	8.30 ± 0.10	8.60 ± 0.05	8.01 ± 0.05	8.04 ± 0.14	7.98 ± 0.05
Oxygen (mg L^{-1})	8.57 ± 0.31	8.27 ± 0.15	8.46 ± 0.12	9.35 ± 0.15	10.39 ± 0.32	9.76 ± 0.05
$NO_2^- + NO_3^- + NH_4^+$ (µM)	4.90 ± 1.64	6.53 ± 0.23	2.33 ± 0.37	7.42 ± 0.03	6.60 ± 0.16	6.46 ± 0.33
PO_4^{3-} (µM)	1.97 ± 0.02	1.76 ± 0.07	0.74 ± 0.13	0.64 ± 0.04	0.52 ± 0.05	0.37 ± 0.16
$Si(OH)_4$ (µM)	3.48 ± 0.02	3.88 ± 0.71	3.11 ± 0.93	2.22 ± 0.01	1.28 ± 0.02	1.51 ± 0.22
POC (mg C m^{-3})	2403 ± 279	3359 ± 151	4552 ± 17	3070 ± 76	2336 ± 250	4554 ± 84
Chl *a* (mg m^{-3})	4.73 ± 0.10	3.66 ± 0.04	3.31 ± 0.10	16.86 ± 0.21	5.45 ± 0.21	4.91 ± 0.13
% Microphyt	31 ± 2	43 ± 3	29 ± 3	21 ± 3	53 ± 5	38 ± 2
% Nanophyt	36 ± 1	27 ± 3	32 ± 5	14 ± 1	22 ± 3	34 ± 2
% Picophyt	33 ± 5	40 ± 3	39 ± 5	65 ± 5	25 ± 2	28 ± 5
Bacterioplankton (mg C m^{-2})	39 ± 4	151 ± 12	234 ± 17	149 ± 17	581 ± 37	268 ± 30
Total phytoplankton (mg C m^{-2})	1081 ± 30	561 ± 20	315 ± 8	900 ± 18	722 ± 30	237 ± 4
% Microphyt	67 ± 3	79 ± 2	68 ± 2	52 ± 2	63 ± 2	61 ± 2
% Nanophyt	25 ± 2	12 ± 0.5	24 ± 1	12 ± 1	28 ± 1	26 ± 2
% Picophyt	8 ± 0.5	9 ± 0.2	8 ± 0.5	36 ± 2	9 ± 0.5	13 ± 1
> 2 µm phytoplankton (mg C m^{-2})	996 ± 42	513 ± 26	290 ± 6	580 ± 26	651 ± 25	205 ± 4
% Auto. ciliates	3 ± 0.5	3 ± 0.7	8 ± 1	6 ± 1	4 ± 0.6	9 ± 1
% Auto. dinoflagellates	20 ± 3	14 ± 3	30 ± 2	28 ± 3	40 ± 3	23 ± 2
% Diatoms	52 ± 3	72 ± 4	38 ± 1	22 ± 2	43 ± 3	39 ± 2
% Phytoflagellates	25 ± 2	11 ± 0.3	24 ± 1	44 ± 3	13 ± 1	29 ± 4
< 2 µm phytoplankton (mg C m^{-2})	85 ± 3	48 ± 2	25 ± 2	320 ± 8	71 ± 2	32 ± 1
% Eukaryotes	80 ± 2	77 ± 3	93 ± 1	20 ± 6	70 ± 2	71 ± 3
% *Synechococcus*	20 ± 2	23 ± 3	7 ± 1	80 ± 6	30 ± 2	29 ± 3
Micozooplankton (mg C m^{-2})	1722 ± 68	517 ± 66	842 ± 18	3372 ± 571	9039 ± 970	393 ± 18

variation, St1 and St2 were characterised by high PO_4^{3-} concentrations, while St3 was distinguished by high POC levels during the two seasons (Table 1, ANOVA, $p < 0.05$, $N = 18$). It should be noted that Chl *a* reached a very high level in St1 during the fall (Table 1, ANOVA, $p < 0.01$, $N = 18$).

During spring, the three size fractions of phytoplankton contributed almost equally to total Chl *a* in all stations (Table 1). During fall, the pico-sized Chl *a* fraction dominated in St1 (65%) whereas the microphytoplankton formed the half of Chl *a* in St2. In St3, the nano- and micro-sized fractions together contributed the most to total Chl *a* concentration.

Carbon biomass, growth and production of bacterioplankton

In general, the carbon biomass of bacterioplankton was significantly lower in spring (39–234 mg C m^{-2}) compared to fall (149–581 mg C m^{-2}) (Table 1, ANOVA $p < 0.01$, $N = 18$). During spring, the bacterial biomass increased from St1 to St3. In fall, it showed the lowest and the highest value at St1 and St2, respectively. Rates of bacterial growth and production (BP) measured in spring (0.82–1.71 d^{-1} and 129 – 470 mg C m^{-2} d^{-1}) were lower than those recorded in fall (1.63–2.50 d^{-1} and 380–1337 mg C m^{-2} d^{-1}) (Table S1, Fig. 3a, ANOVA $p < 0.01$, $N = 18$). The lowest growth and production rates recorded were found at St1 and the highest were found at St2 in spring, while rates decreased from St1 to St3 in fall. The bacterial production followed the spatial and seasonal variations of total phytoplankton production ($r_s = 0.78$, $p < 0.01$, $N = 18$).

Carbon biomass, growth and production of phytoplankton

Total carbon biomass of phytoplankton showed significant variations between seasons and stations (Table 1, ANOVA, $p < 0.01$, $N = 18$). During each season, the highest biomasses were recorded at St1 and the lowest biomasses in St3. Phytoplankton biomass was dominated by > 2-µm-sized

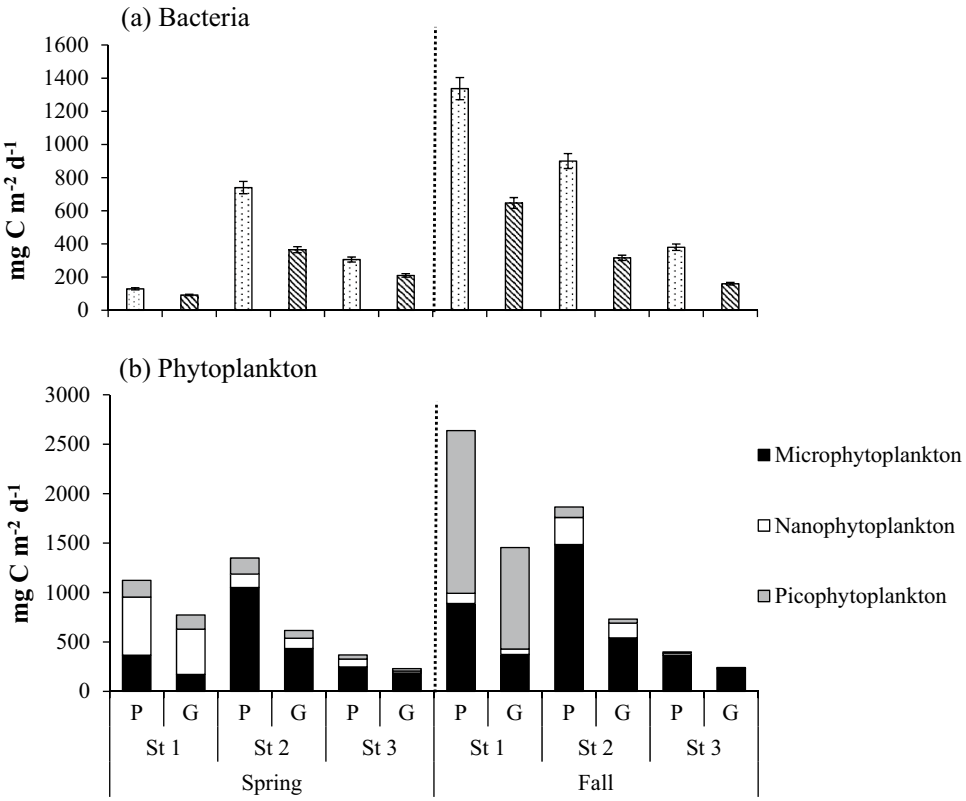

Fig. 3 Production (*P*) and consumption (*G*) rates of **a** bacterioplankton and **b** phytoplankton (three size fractions) in the study stations during the spring and fall 2017 (mean values ± SD)

cells, specifically by the micro-sized fraction (55–80%). The > 2 µm phytoplankton showed significantly variable biomasses among seasons and stations (205–996 mg C m^{-2}, Table 1, ANOVA, $p < 0.01$, $N = 18$). Micro-sized diatoms dominated the > 2 µm phytoplankton biomass at all stations during spring (38–72%, Table 1) and were mostly represented by larger species (45–105 µm), such as *Lithodesmium undulatum, Dactyliosolen fragilissimus* and *Licmophora flabellate*. During fall, diatoms showed a large decrease at St1 (only 22% of > 2 µm phytoplankton biomass), whereas nano-sized phytoflagellates (mainly chlorophyceae *Mamiella gilva*) became dominant (44%). Diatoms remained an important component of the > 2 µm phytoplankton during fall at St2 and St3 (39–43%), with *Skeletonema costatum* and *Navicula* spp. (12–30 µm) as dominant species. Autotrophic dinoflagellates (represented by *Prorocentrum compressum*, *P. gracile* and *P. lima*) contributed 14–30% to the community in spring and 23–40% in fall. Autotrophic ciliates (*Mesodinium rubrum*) were scarce, accounting for only 3–9% of the community (Table 1). Carbon biomass of picophytoplankton varied largely from 25 to 320 mg C m^{-2} (Table 1, ANOVA, $p < 0.01$, $N = 18$). The picoeukaryotes were dominant during spring at all stations, forming 56–85% of pico-sized carbon biomass. During fall, picoeukaryotes and *Synechococcus* showed similar contributions at St2 (51 and 49%) and St3 (48 and 52%), while *Synechococcus* displayed a pronounced biomass at St1 (253 mg C m^{-2}) and hence, formed 80% of the picophytoplankton biomass. Accordingly, the pico-sized fraction, which did not exceed 12% of total phytoplankton carbon throughout the study, showed an increased contribution (~ 40%) at St1 during fall. A significant positive correlation was found between the *Synechococcus* biomass and N-nutrient levels ($r_s = 0.48$, $p < 0.05$).

The growth rate of each phytoplankton size fraction varied significantly (ANOVA $p < 0.01$, $N = 18$) between seasons and stations (Table S1). During both seasons, the highest growth rates for picophytoplankton were observed at St1, with a decreased value in spring (1.5 d^{-1}) relative to fall (2.9 d^{-1}). At the other stations, growth rates of pico-sized fraction were somewhat higher in spring (0.44–1.22 d^{-1}) than in fall (0.26–1.01 d^{-1}). For nanophytoplankton, growth rates ranged from 0.55 to 1.88 d^{-1} in spring and generally decreased in fall (0.21–1.01 d^{-1}). An opposing pattern was observed for microphytoplankton, which showed relatively higher growth rates in fall (0.85–1.76 d^{-1}) than in spring (0.70–1.25 d^{-1}). For all size fractions, growth rates measured at St3 were significantly lower than those recorded at other stations during both seasons (ANOVA $p < 0.01$, $N = 18$).

Size-fractioned and total phytoplankton production (PP) varied significantly among stations and seasons (Fig. 3b, ANOVA, $p < 0.01$, $N = 18$). Picophytoplankton had a very high production rate during fall at St1 (1646 mg C m^{-2} d^{-1}), while lower values were recorded at the other stations

during both seasons (13–169 mg C m^{-2} d^{-1}). Production rates for nanophytoplankton were in general low (20–270 mg C m^{-2} d^{-1}) but increased during spring at St1 (588 mg C m^{-2} d^{-1}). Microphytoplankton production rates in spring (248–1051 mg C m^{-2} d^{-1}) were relatively lower compared to fall (366–1500 mg C m^{-2} d^{-1}). During both seasons, the highest and the lowest values were measured at St2 and St3, respectively. Total PP rates measured in spring (1123–1349 mg C m^{-2} d^{-1}) were lower than in fall (1865–2638 mg C m^{-2} d^{-1}) at St1 and St2, while similar and lower rates (369–399 mg C m^{-2} d^{-1}) were recorded at St3 during both seasons. During spring, total PP was sustained mainly by the nano-sized fraction at St1 (52%) and by the micro-sized fraction at St2 and St3 (70%). During fall, the picophytoplankton largely dominated the carbon production at St1 (65%), while most of PP at St2 and St3 were driven by microphytoplankton (80–92%) (Fig. 3b).

Microzooplankton biomass, composition and grazing activity

Microzooplankton biomass showed spatial and seasonal heterogeneity (Table 1, ANOVA, $p < 0.01$, $N = 18$). Biomasses recorded during spring, at St1 (1722 mg C m^{-2}) and St2 (517 mg C m^{-2}), were very low compared to those observed in fall (3372 and 9039 mg C m^{-2}), while at St3, the biomass in spring (842 mg C m^{-2}) exceeded that in fall (393 mg C m^{-2}). The microzooplankton community composition also changed between seasons and stations (Fig. 4). During spring, the community was composed mainly by HNF, HDino and MDino that represented 19–39, 16–31 and 34–39% of total microzooplankton biomass, respectively (Fig. 4a). In all stations, HNFs were dominated by small species (< 10 µm) of *Leucocryptos*, and HDino were composed essentially by species of *Gyrodinium* (66–90%, Fig. 4b), while MDino were mainly represented by *Prorocentrum minimum* (54–78%, Fig. 4c). In fall, MDino contributed largely to the microzooplankton biomass (44–81%), no matter the station. They were dominated by *P. minimum* at St1 (84%) and by *Karenia selliformis* at St2 (97%), while *Gymnodinium* and *Heterocapsa* were the main genera at St3 (67%). HDino, which contributed ~ 20% of microzooplankton biomass, consisted primarily of *Gyrodinium* species at St2 (95%), but *Podolampas palmipes* was dominant at St1 (60%), while several species, such as *Gyrodinium*, *Oxytoxum* and *P. palmipes*, composed the HDino at St3 (Fig. 4b). Overall, aloricate ciliates, mainly *Strombidium* spp., and tintinnids, mainly *Tintinnopsis* spp., contributed little to the community (0–7 and 2–13%, respectively). Mixotrophic nanoflagellates (MNF), which were observed only in fall, accounted for 1–12% of microzooplankton biomass.

Grazing and consumption rates by microzooplankton for bacterioplankton and phytoplankton size fractions varied significantly between seasons and stations (Table S1, Fig. 3a, b, ANOVA, $p < 0.01$, $N = 18$). For each food item, consumption rates tracked the variation of production rates, with significant positive correlations between both rates ($r_s = 0.75$ for bacteria, $r_s = 0.97$ for phytoplankton, $p < 0.001$). For bacterioplankton, grazing rates and consumption rates measured in spring did not vary so much during fall at St2 and St3, while they largely increased at St1 (Fig. 3a, Table S1). Grazing and consumption rates on picophytoplankton measured in St2 and St3 were higher in spring than in fall while an inverse trend was observed at St1. Overall, feeding rates on nanophytoplankton did not vary much, but increased during spring at St1. Microphytoplankton was grazed at relatively lower rates in spring than in fall (Fig. 3b, Table S1). Microzooplankton grazing impact on BP ranged from 50 to 72% in spring and from 35 to 50% in fall. During spring, the micrograzers daily consumed significant proportions of PP from pico-, nano- and micro-sized fractions at all stations (50–86, 25–78 and 50–74%, respectively). During fall, the microzooplankton daily removed 62% of picophytoplankton production at St1 but no more than 40% at the other stations. The microzooplankton grazing corresponded to a daily removal of 40–62% of the microphytoplankton production and 45–54% of the nanophytoplankton production.

The *co-inertia* analysis was applied on the two tables with the same lines (stations and seasons) and in columns the consumption rates of the different prey versus the biomass of their potential microzooplankton grazers. These two tables presented a total *co-inertia* of 57%, showing a strong link between structure of these two tables (Fig. 5). The biomasses of *K. selliformis* and *Gyrodinium* spp. were linked with the consumption rate of microphytoplankton. *Prorocentrum minimum* biomass appeared to be linked with the grazing of bacterioplankton and picophytolankton. The consumption of nanophytoplankton was linked with the biomasses of *Strombidium* spp. and *Leucocryptos sp*. These links were confirmed by Spearman positive correlations between the biomasses of the microzooplankton taxa and the consumption rates, suggesting potential prey-predator relationships (Fig. S2). The mixotrophic *P. minimum* showed positive correlations with the consumption rates of picophytoplankton and bacterioplankton ($r_s = 0.68$–0.74, ANOVA, $p < 0.01$). The consumption of microphytoplankton presented a positive relationship with the MDino *K. selliformis* ($r_s = 0.74$, $p < 0.01$) and the HDino *Gyrodinium* spp. ($r_s = 0.69$, $p < 0.05$). The consumption of nanophytoplankton was positively related with the HNF *Leucocryptos* and the aloricate ciliates *Strombidium* spp. ($r = 0.57$–0.66, $p < 0.05$).

Mesozooplankton abundance, composition and grazing activity

Mesozooplankton abundance varied significantly between seasons and stations, ranging from 1.15 to 6 10^3 ind m^{-3}

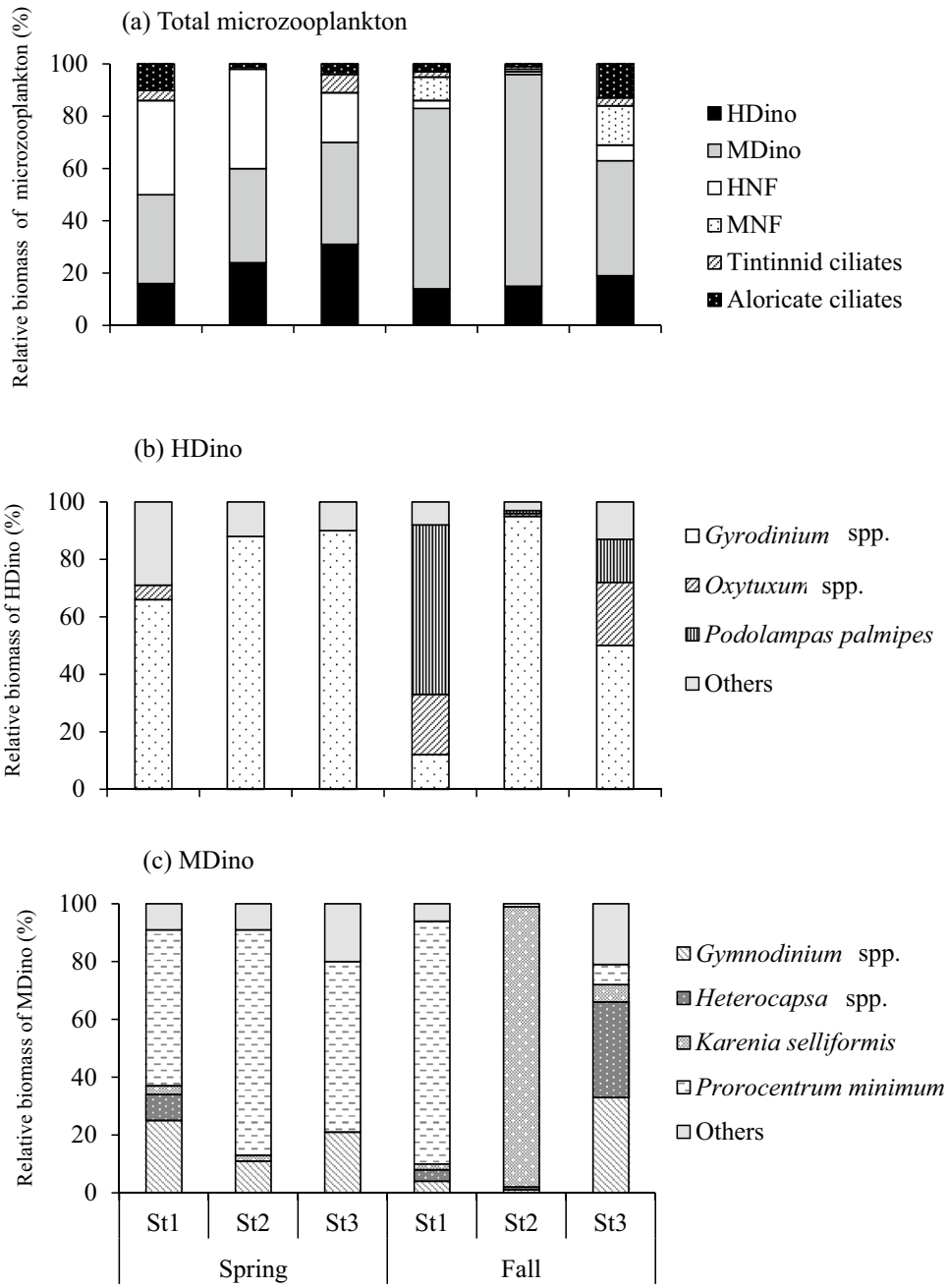

Fig. 4 Composition of total microzooplankton, heterotrophic and mixotrophic dinoflagellates (HDino, MDino) in the study stations during the spring and fall 2017

in most samples, but reached high values during fall in St2 (26.83 10^3 ind m^{-3}) (Table 2, ANOVA, $p < 0.05$, $N = 18$). Copepods were dominant (83–97% of total abundance) and included mostly herbivorous calanoida (27.8–94.5%, mainly *Calanus*, *Centropages* and *Acartia*) and cyclopoida (2.4–33.3%, mainly *Cyclopina*). The exception was St1 in fall, where the detritivorious *Euterpina acutifrons* (harpacticoida; Greve et al. 2004) contributed 53% of copepod abundance.

Grazing rates by mesozooplankton on phytoplankton, which varied over seasons and stations (Table 2, ANOVA, $p < 0.01$, $N = 18$), were positively correlated with the production rates of both nano- and micro-sized fractions ($r_s = 0.66$–0.75; $p < 0.01$). During spring, higher grazing rates were recorded at St1 and St2 compared to St3. Mesozooplankton removed 13–15% of PP and 14–56% of standing crop daily. During fall, mesozooplankton grazing strongly increased at St2, reaching higher rates relatively to other stations. Mesozooplankton only consumed 7% Chl *a* d^{-1} and 4% P d^{-1} at St1. However, higher impact was observed at St3 (12% P grazed d^{-1} and 42% Chl *a* grazed d^{-1}) and the highest was observed at St2 (25% P grazed d^{-1} and 70% Chl *a* grazed d^{-1}).

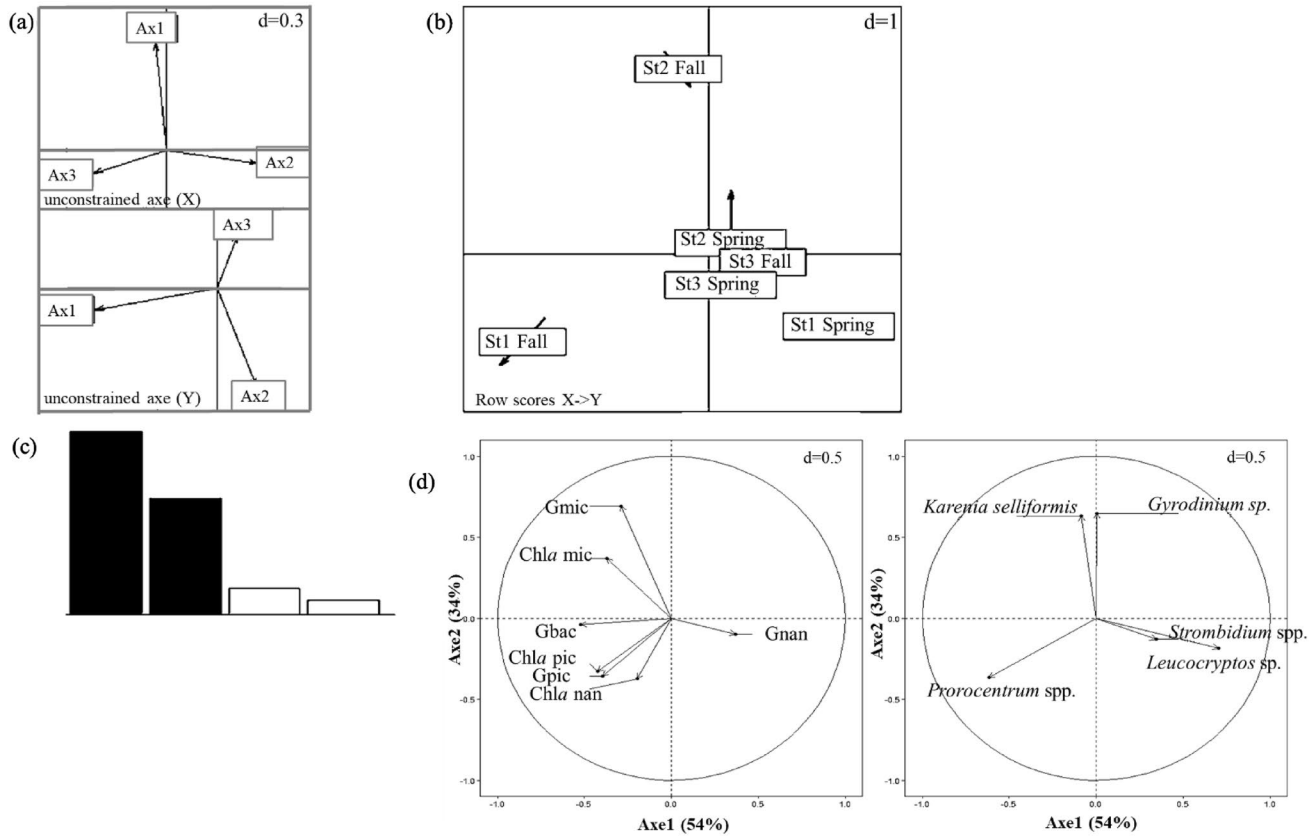

Fig. 5 Plot of a co-inertia analysis: projection of the principal axes of the two tables. One table is the consumption rates of preys per station and season, the second the biomass of micrograzers per station and season, on co-inertia axes. **a** Unconstrained axes (*x*, *y*), **b** Joint display of the sites, **c** Eigenvalues screeplot and **d** Canonical weights of preys and predators

Mesozooplankton predation on microzooplankton was significantly different between seasons (ANOVA, $p < 0.01$). Similar feeding rates were determined at all stations during spring (324 – 395 mg C m^{-2} d^{-1}), while during fall, mesozooplankton showed higher predation on microzooplankton at St1 (525–787 mg C m^{-2} d^{-1}) compared to St2 and St3 (150–393 mg C m^{-2} d^{-1}).

Exportation of carbon

During spring, the rate of carbon potentially transferred to higher consumers in all stations varied from 52 to 214 mg C m^{-2} d^{-1}, which represented 11–22% of PP. The rate of carbon sedimentation could reach 92–539 mg C m^{-2} d^{-1}, representing 25–40% of PP. During fall, 6–13% of PP, corresponding to 175–350 mg C m^{-2} d^{-1}, could be provided to higher consumers in St1, while higher fraction of PP (12–25%) was potentially available for predators in St2 and St3. Similarly, the rate of sedimentation in St1 (490 mg C m^{-2} d^{-1}) represented a lower fraction of PP (18%) than in St2 and St3 (26–37%; 107–690 mg C m^{-2} d^{-1}).

Discussion

Trophic condition, productivity and microbial community

The Gulf of Gabès was characterised by eutrophic conditions. Indeed, high nutrient concentrations were recorded during all sampling periods (Table 1), particularly for PO_4^{3-} (0.37–1.97 µM), which exceeded those generally reported for other Mediterranean coastal waters, such as the Gulf of Lion (0.06–0.12 µM) and Lagoons of Thau (0.18 µM) or Mar Menor (0.09–0.23 µM) (Ross et al. 2016; Courboulès et al. 2021; Mercado et al. 2021). Chl *a* concentrations measured during the study (3.7–16.9 mg m^{-3}) were in the range of those found in eutrophic coastal waters, such as the Gulf of Trieste (0.4–5.9 mg m^{-3}), Bizerte Lagoon (2.2–8.8 mg m^{-3}) and Thau Lagoon (0.4–5.4 mg m^{-3}) (Fonda Umani and Beran 2003; Bec et al. 2005; Meddeb et al. 2018). The size structure of phytoplankton confirms the eutrophic characters of the study site, since large phytoplankton (> 2 µm cells: nano- and micro-sized fractions) dominated the Chl *a* (60–75%), carbon biomass (87–92%)

Table 2 Abundances, composition, grazing rates and grazing impact of mesozooplankton and microzooplankton in the study stations during the spring and fall 2017

	Spring			Fall		
	St1	St2	St3	St1	St2	St3
Abundance (10^3 ind m^{-3})						
Mesozooplankton	6.00 ± 1.12	2.25 ± 0.43	5.07 ± 0.50	3.76 ± 1.12	32.03 ± 3.67	1.15 ± 0.61
Copepods	5.43 ± 1.06	2.17 ± 0.40	4.91 ± 0.42	3.59 ± 1.04	26.80 ± 1.76	1.02 ± 0.50
% Total abundance						
Copepods	92.97 ± 0.25	96.44 ± 0.55	96.82 ± 0.47	93.97 ± 2.14	82.57 ± 1.57	90.39 ± 5.27
Others	7.03 ± 0.25	3.56 ± 0.55	3.18 ± 0.47	6.03 ± 2.14	17.43 ± 1.57	9.61 ± 5.27
% Copepods abundance						
Calanoida	72.99 ± 0.26	94.47 ± 2.15	75.23 ± 1.00	27.83 ± 12.75	79.36 ± 1.32	31.80 ± 0.31
Acartia	4.55 ± 0.49	65.31 ± 3.00	6.12 ± 1.30	3.83 ± 1.50	15.10 ± 2.92	9.35 ± 8.87
Calanus	50.08 ± 1.49	3.00 ± 0.34	65.75 ± 1.20	9.96 ± 11.14	27.48 ± 0.77	18.56 ± 8.57
Centropages	13.03 ± 1.17	n.o	0.97 ± 0.28	n.o	34.93 ± 2.21	n.o
Eucalanus	1.87 ± 0.02	1.67 ± 0.33	0.40 ± 0.60	n.o	0.18 ± 0.12	n.o
Isias	n.o	n.o	0.41 ± 0.16	n.o	n.o	n.o
Paracalanus	0.90 ± 0.81	19.23 ± 0.34	0.26 ± 0.36	14.04 ± 0.07	n.o	n.o
Phaenna	0.69 ± 0.06	2.33 ± 0.30	0.54 ± 0.34	n.o	n.o	n.o
Microcalanus	0.53 ± 0.29	1.33 ± 0.36	0.52 ± 0.74	n.o	0.32 ± 0.04	n.o
Temora	1.34 ± 0.53	1.60 ± 0.46	0.26 ± 0.37	n.o	1.35 ± 0.55	3.89 ± 3.33
Cyclopoida	23.00 ± 0.75	2.43 ± 1.36	7.77 ± 0.73	9.17 ± 0.88	2.71 ± 1.28	33.34 ± 4.79
Cyclopina	16.41 ± 2.42	0.83 ± 0.17	5.82 ± 0.89	6.56 ± 1.11	2.26 ± 0.49	31.01 ± 0.34
Oithona	6.59 ± 1.08	1.60 ± 0.46	1.95 ± 0.56	2.61 ± 0.23	0.45 ± 0.23	2.33 ± 1.12
Harpacticoida	1.59 ± 0.87	3.24 ± 0.80	16.31 ± 1.91	57.55 ± 5.62	15.24 ± 0.42	33.32 ± 2.92
Euterpina	1.59 ± 0.87	1.00 ± 0.30	10.33 ± 0.09	52.79 ± 15.81	5.51 ± 1.65	21.71 ± 0.24
Harpacticus	n.o	2.50 ± 0.50	5.45 ± 1.48	4.58 ± 0.05	9.36 ± 1.51	8.51 ± 3.20
Tegastidae	n.o	n.o	n.o	0.17 ± 0.25	n.o	n.o
Stylicletodes	n.o	n.o	0.54 ± 0.34	n.o	0.37 ± 0.28	3.10 ± 0.03
Copepodites	2.36 ± 0.13	n.o	0.70 ± 0.25	5.46 ± 2.17	2.71 ± 0.47	1.54 ± 2.18
Mesozoo. grazing rates (mg C m^{-2} d^{-1})	145.45 ± 35.05	177.13 ± 2.39	41.32 ± 14.31	45.58 ± 10.98	432.35 ± 26.69	47.83 ± 5.75
Mesozoo grazing impact						
%P grazed d^{-1}	15.13 ± 3.05	14.97 ± 1.07	12.97 ± 5.64	4.69 ± 1.60	25.00 ± 0.54	12.40 ± 1.24
% Chl *a* grazed d^{-1}	14.00 ± 3.36	56.00 ± 1.02	27.50 ± 13.47	7.22 ± 1.74	70.48 ± 6.15	42.00 ± 5.00
Microzoo grazing impact						
%P grazed d^{-1}	68.87 ± 2.72	45.57 ± 6.88	62.27 ± 5.35	55.55 ± 5.46	39.24 ± 4.21	60.55 ± 7.54

n.o not observed, $N = 18$

and primary production (84–96%) during the sampling campaign.

Our study provided the first estimation of PP rates in the Gulf of Gabès, based on the growth rates determined from the dilution experiments, as already performed in other environments (Moigis and Gocke 2003; Sakka Hlaili et al. 2008; Meddeb et al. 2018; Dokulil and Qian 2021). Nutrients were not added into our dilution bottles since we assumed that N and P were available in the Gulf year-round (Bel Hassen et al. 2008, 2009). Furthermore, several authors found that nutrients have no effect of phytoplankton growth during the dilution experiments when conducted in eutrophic systems (Sakka Hlaili et al. 2007; Pecqueur et al. 2022). Our growth rate estimates were in the range of rates measured from the dilution experiments (with or without nutrient additions) in other coastal waters (Bec et al. 2005; Grinienė et al. 2016). Overall, our PP rates (369–2638 mg m^{-2} d) (Fonda Umani and Beran 2003[1]) were high and comparable with estimates from the dilution method in coastal environments, such as in the Gironde Estuary (525–746 mg C m^{-2} d^{-1}; Sautour et al. 2000), the Rhode River Estuary, the Kiel Fjord (701–1008 mg C m^{-2} d^{-1}; Moigis and Gocke 2003) and the Bizerte Lagoon (435–1779 mg C m^{-2} d^{-1}; Grami et al. 2008). The high trophic conditions and the high productivity

of the Gulf associated with the nutrient availability disagrees with the well-known Eastern Mediterranean Basin oligotrophy. This suggests that the singularity of this coastal ecosystem has been subjected to various influences from anthropogenic sources and Saharan dust, which may contribute to the nutrient enrichment of the Gulf (Drira et al. 2009; Hamza et al. 2016; Khammeri et al. 2018). Bacterial production rates were also high and closely associated to PP rates ($r_s = 0.783$, $p < 0.01$), suggesting a tight coupling between BP and PP. This is expected since most carbon needed by bacterioplankton is provided by phytoplankton exudates (Duarte and Agusti 2005; Ning et al. 2005). Our estimates of bacterial growth (0.82–2.5 d^{-1}) and production rates (128–1337 mg C m^{-2} d^{-1}) were in the upper range reported for other coastal areas (Vargas et al. 2007; Grami et al. 2008; Courboulès et al. 2021; Pecqueur et al. 2022).

Total Chl *a*, PP and BP were generally lower in spring than fall, which could be related to the different nutrient conditions between both seasons (Table 1; Fig. 3a, b). Indeed, the fall was characterised by higher concentrations of N-nutrients and more suitable nutrient conditions for phytoplankton proliferation (i.e. N:P ~ 16). The sampling stations were located in shallow areas (maximal depth < 15 m), where turbulent vertical mixing was important due to the tide dynamics (Sammari et al. 2006) and also to the wind forcing known to be particularly active during this season, leading to sediment re-suspension and nutrient release. During fall, this ecosystem was shown to be particularly rich with organic matter and remineralising heterotrophic bacteria (Quéméneur et al. 2020), which constitute potential sources of regenerated nutrients.

The large phytoplankton displayed a clear variation in species composition between spring and fall (Table 1). The most important change concerned the contribution of large micro-sized diatoms (such as *Lithodesmium undulatum, Dactyliosolen fragilissimus* and *Licmophora flabellate*), which were generally more abundant during spring than in fall, as was previously reported in the Gulf (Bel Hassen et al. 2008). The spring abundance of large diatoms is likely a common feature of the coastal Mediterranean waters, as in the Lagoon of Bizerte, Gulf of Naples and Gulf of Lions (d'Alcalà et al. 2004; Meddeb et al. 2018; Leblanc et al. 2018).

A spatial heterogeneity in the phytoplankton community structure was pointed out mainly during fall. At this period, St1 was clearly distinguished from other stations with a picophytoplankton having the highest contribution to Chl *a* and PP (65%) and very high growth rate (2.9 d^{-1}) and biomass (320 mg C m^{-2}), coinciding with a high dominance of *Synechococcus* (Table 1; Fig. 3b). This station is located in a region where recurrent cyanobacteria blooms have been reported, which correlates with the high N-nutrient accumulations from Saharan dust (Hamza et al. 2016). In our study, *Synechococcus* biomass showed a positive correlation with inorganic N ($r_s = 0.477$, $p < 0.05$), confirming the general trend observed in other Mediterranean areas where *Synechococcus* was abundant in nutrient-rich and well-mixed waters (Šantić et al. 2011; Quéméneur et al. 2020). Our findings highlight that small phytoplankton (< 2 µm) play an important functional role in the South Mediterranean system that is characterised by high trophic conditions. St 3 was distinguished by low biomass and PP during both seasons (Table 1; Fig. 3b), probably because of lower N and P nutrient concentrations than in the other stations (Table 1). Furthermore, St3 is located within an area that is strongly impacted by heavy metals released from the chemical industry (Fig. 1), which could affect the phytoplankton metabolism and physiology (Liu et al. 2017; Deng et al. 2020), causing a decrease in growth rates for all size fractions (Table S1) and hence a decrease in phytoplankton biomass and production.

Ecological role of microzooplankton

The ecological role of microzooplankton has been scarcely reported for the South Mediterranean systems (Sakka Hlaili et al. 2007; Meddeb et al. 2018), and little is known about its contribution to the functioning of the Gulf of Gabès. During our study, microzooplankton reached a high biomass (Table 1) that exceeded estimates reported for other coastal regions (Vargas et al. 2007; Sakka Hlaili et al. 2008; Calbet et al. 2012), suggesting that microzooplankton could be a major grazer in the Gulf. The grazing rates for different phytoplankton size fractions ranged between 0.14 and 1.9 d^{-1}, which compares with estimates reported for fractioned phytoplankton from dilution method in others coastal regions, such as Chesapeake Bay (0.41–1.92 d^{-1}), Curonian Lagoon (1.52–1.83 d^{-1}) and Thau Lagoon (0.2–0.6 d^{-1}) (Sun et al. 2007; Grinienė et al. 2016; Pecqueur et al. 2022). Grazing rates for bacterioplankton (0.53 and 1.7 d^{-1}) were also consistent with values reported by other studies using the dilution technique (Courboulès et al. 2021; Pecqueur et al. 2022). The grazing rates could be overestimated in the dilution experiment without nutrients if phytoplankton growth was limited (Landry and Hassett 1982). During our study, nutrients were not added, but as discussed before, the phytoplankton growth was kept in suitable nutrient condition during our experiment. The grazing impact of microzooplankton on total phytoplankton estimated in our study (39–68% P grazed d^{-1}) was within the ranges of the values (> 60% of PP) reported for several coastal ecosystems (Aberle et al. 2007; Calbet 2008; Aytan et al. 2018), but higher than those reported for some near shore waters (≤ 40%; Meddeb et al. 2018). During our work, microzooplankton displayed a higher top-down control on

total phytoplankton than mesozooplankton, which grazed only ~ 5–25% P d^{-1} (Table 4). Our results reinforce the idea that protozoan organisms are the most important grazers in various marine environments (Calbet and Landry 2004; Vargas et al. 2007; Meddeb et al. 2018; Romano et al. 2021).

The grazing activity of microzooplankton varied significantly between seasons and stations (Table S1; Fig. 3a, b), likely in response to the variation in the growth of prey (Gentleman et al. 2003; Sandhu et al. 2019). The consumption rate of each prey was indeed positively correlated to its production rate ($r = 0.75–0.97$, $p < 0.001$). Changes in the microzooplankton community structure can also largely influence the grazing activity, as different protozoan groups have selective feeding (Takashi and Satoshi 2001). In spring, microzooplankton showed similar compositions (Fig. 4) and exerted similar grazing pressure on each prey between stations. They consumed significant proportions of picophytoplankton and bacterial production whatever the station (50–72 and 50–82%, respectively). The consumption of these pico-sized prey may be assigned to the HNF (Calbet and Landry 2004; Berglund et al. 2007), which were an important component of microzooplankton in spring (20–40%, Fig. 4a) and to the dominant MDino *P. minimum* (54–78%, Fig. 4c), which is known to feed on very small preys (Jeong et al. 2005, 2010). Potential prey-predator relationships between bacterioplankton or picophytoplankton and *P. minimum* were shown by *co-inertia* and Spearman correlation analyses (Fig. 5, Fig. S2). Nanophytoplankton was also under significant grazing pressure (25–78% P grazed d^{-1}), which seemed due to aloricate ciliates (i.e. *Strombidium* spp.) and HNF (i.e. *Leucocryptos sp.*) (Figs. 5, S2), as reported in other marine systems (Šimek et al. 1995; 2000; Sato et al. 2007). Microphytoplankton (Figs. 5, S2), which was under high grazing control by microzooplankton (50–74% P grazed d^{-1}), seemed to be mainly controlled by the HDino *Gyrodinium* spp. (Figs. 5, S2), which are known as diatom consumers (Saito et al. 2006; Jeong et al. 2010). In fall at St1, *P. minimum* was dominant and *Gyrodinium* decreased in detriment of small diatom consumers, such as *Oxytoxum* and *Podolampas* (Fig. 4a) (Gomès et al. 2007; Girault et al. 2013; Kase et al. 2021). Therefore, bacterio- and picophytoplankton were largely grazed (> 50% P grazed d^{-1}), while microphytoplankton was under low grazing pressure (40% P grazed d^{-1}). Conversely, the pico-sized prey were weakly exploited (≤ 40% P grazed d^{-1}) at St2 and St3, where microbivorous consumers (such as *P. minimum* and HNF) were scarce. The microphytoplankton at both stations was however under substantial control by microzooplankton (40–62% P grazed d^{-1}), since *Gyrodinium* spp. were well represented and the MDino *K. selliformis*, which also appeared as a potential grazer of microphytoplankton (Figs. 5, S2), was dominant at St2.

Ecological role of mesozooplankton

During all the samplings, the mesozooplankton were clearly dominated by copepods (83–97%, Table 2), as previously reported in the Gulf of Gabès (Drira et al. 2014, 2017; Makhlouf Belkahia et al. 2021) and in other Mediterranean regions (Fonda Umani et al. 2003; Sakka Hlaili et al. 2008; Siokou Frangou et al. 2010; Ben Lamine et al. 2015). Our sampling was carried out during the day, when mesozooplankton is concentrated at the bottom of the water column and expected to have a low feeding rate compared to the night. Despite this, mesozooplankton grazing impacts found in our study (7 and 70% of Chl *a* d^{-1} and from 5 to 25% of P d^{-1}) were in the range of estimates from gut content method in other coastal waters from the Mediterranean (8 and 30% of PP in the Bay of Bizerte; Meddeb et al. 2018) or from other oceanic regions (5 to 40% of P in coastal waters off Plymouth, SW England; Bautista and Harris 1992 and in Gironde estuary; Sautour et al. 2000).

The spatial and seasonal variation in mesozooplankton grazing pressure was linked to the change in the availability and size structure of phytoplankton, which may significantly affect the feeding of copepods (Almeda et al. 2011; Bi and Sommer 2020). This was confirmed by the positive correlation ($r = 0.66–0.75$, $p < 0.01$) between the consumption rate by mesozooplankton and the production of the nano- and microphytplankton, which are known as their potential prey (Chen et al. 2017; Feng et al. 2020). Moreover, feeding rates of mesozooplankton were maximal when micro-sized fraction showed the highest contribution to the Chl *a* biomass and minimal in case of dominance by picophytoplankton, which is not suitable prey for copepods (Berggreen et al. 1988; Morales et al. 1993). Change in the composition of the mesozooplankton community was another factor of the variation in its grazing rate. Detritivorous copepods (i.e. *Euterpina acutifrons*) were very abundant at St1 during fall (53% of copepods, Table 2), when the lowest grazing effect of mesozooplankton was recorded. Conversely, herbivorous calanoida (such as *Acartia*, *Calanus, Paracalanus*, *Eucalanus* and *Centropages*) were preponderant during the other samplings, reaching very high abundance at St2 during fall, where the highest impact of grazing pressure was observed (Table 2).

Food web structure and carbon transfer

The fate of the primary production and the efficiency of the carbon transfer depend largely on the food web structure (Legendre and Rassoulzadegan 1995; Thompson et al. 2012). Thus, determining the typology of PFW is central, particularly in the highly productive coastal areas, which are of socio-economic importance, such as the Gulf of Gabès. Figure 6 presents simplified conceptual PFW for each season

at the three stations, including planktonic compartments with their production rates and trophic links.

During spring, the PFW at all stations was mainly fueled by the production of > 2 µm phytoplankton, which was dominated by micro-sized diatoms and also formed a substantial proportion of Chl *a*. The picophytoplankton contributed ~ 15% of PP and 33–40% of Chl *a*. BP reached 50–83% of PP at most stations and could supply a large amount of carbon into the food web. The high microzooplankton grazing on all food items participated actively in the carbon transfer through the PFW. The dominant herbivorous copepods have relatively important grazing on > 2 µm phytoplankton (13–15% P d^{-1}). The production of microzooplankton (324–395 mg C m^{-2} d^{-1}) can supply a portion of carbon to mesozooplankton. Finally, the production of mesozooplankton (52–214 mg C m^{-2} d^{-1}) was then available to higher pelagic consumers. The diagrams of the trophic interactions showed that the microbivory and herbivory of zooplankton act together in channeling biogenic carbon that was produced by small and large phytoplankton (Fig. 6a), suggesting that multivorous food webs may play a major role during spring at all stations (Legendre and Rassoulzadegan 1995). Our results are different from the traditional view, stipulating that the herbivorous pathway usually prevails during the spring with the dominance of large diatoms. Nevertheless, Meddeb et al. (2018) have recently observed a multivorous food web in a coastal Mediterranean Lagoon in spring, when diatoms were dominant.

Unlike spring, different PFWs were observed during fall. The PFW at St1 mainly relied on the high production of picophytoplankton and bacterioplankton. The small microbivorous microzooplankton play a key role in carbon transfer, since herbivorous protozoans and metazoans were scare and showed low grazing impact on large phytoplankton

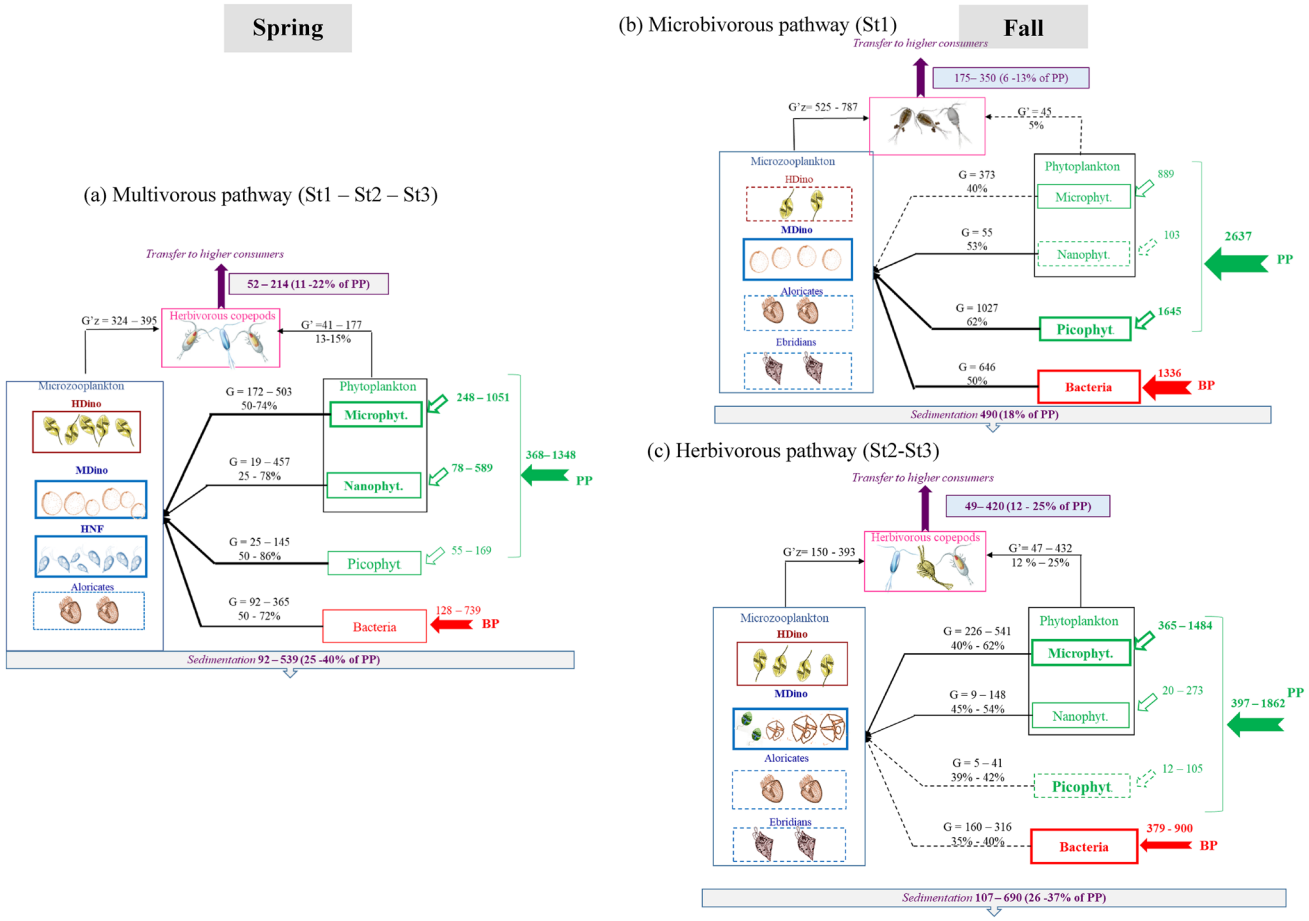

Fig. 6 Conceptual trophic pathways proposed for the study stations during the spring and fall 2017. Primary production (*PP*), bacterial production (*BP*), consumption by microzooplankton (*G*) and mesozooplankton (*G'*) are expressed in mg C m^{-2} d^{-1}. Percentages given with arrows represent the fractions of PP or BP consumed per day. Widths and type of arrows (dashed or solid) indicate magnitude of carbon rate (solid arrows with large width indicate a strong magnitude of carbon rate; dashed arrows with small width indicate a small magnitude of carbon rate). The thickness of phytoplankton boxes is proportional to the production rate (*P*) of each size fraction (wide line = high rate, less wide line = moderate rate, dashed line = low rate). The thickness of microzooplankton boxes is proportional to the abundance of the protozoan group (solid line = abundant group, dashed line = scarce group)

(Fig. 6b). This suggests that the microbial pathway was dominant (Legendre and Rassoulzadegan 1995). This situation corroborates with other findings of microbial carbon pathways in eutrophic coastal regions (Grami et al. 2008; Pecqueur et al. 2011; Viñas et al. 2013; Paklar et al. 2020). In contrast, the herbivorous pathway seemed to dominate at St2 and St3 (Fig. 6c), where diatoms were abundant and the microphytoplankton contributed the most to PP (80–92%). The biogenic carbon was mainly channeled by the herbivorous microzooplankton and mesozooplankton. The herbivorous pathway was also reported during fall in other Mediterranean areas, such as the Catalan Sea (Calbet et al. 1996) and the Southwestern Mediterranean Sea (Meddeb et al. 2018).

The seasonal and spatial changes in the PFW structure suggest that the biogenic carbon would be channeled to higher consumers with a different efficiencies. A significant proportion of PP could be available to higher pelagic consumers during spring (11–22% at all stations) and fall (12–25% at St2 and St3), when multivorous and herbivorous pathways were prevailing (Fig. 6a, c). In both food webs, a significant fraction of PP ($\geq$25%) could also be potentially exported through the sedimentation of large phytoplankton and/or faecal pellets of mesozooplankton. These particles have an important nutritional value, particularly for herbivorous copepods (Dagg et al. 2014), and therefore could fuel the benthic food web by participating in the exportation of PP. This agrees with previous studies showing that PP is efficiently exported throughout herbivorous and multivorous food webs (Legendre and Rassoulzadegan 1995; Meddeb et al. 2019). Conversely, in microbial food webs, most of the carbon is recycled and inefficiently transferred to higher trophic levels (Legendre and Rassoulzadegan 1995; Decembrini et al. 2009). This is consistent with the microbial pathway observed at St1 during fall, which provided only 6–13% of PP to higher consumers and where 18% of PP were potentially exported through sedimentation (Fig. 6b). However, considering the high PP at St1 during fall (mainly from picophytoplankton) and the high feeding of microzooplankton, a large amount of carbon was channeled to mesozooplankton and then to higher consumers (175–350 mg C m^{-2} d^{-1}). This quantity of carbon, although it only represented 6–13% of PP at St1, did not differ so much from the amount of carbon exported via the herbivorous food web at St2 and St3 during the same season (49–420 mg C m^{-2} d^{-1}). Our results reaffirm the crucial role of microzooplankton (including heterotrophic and mixotrophic organisms) in channeling carbon when mesozooplankton have low herbivorous activity and suggest that carbon channeled by the microbial food web may be considerably consistent, particularly in highly productive coastal regions. Further modelling studies should be performed while considering all planktonic processes (production, respiration excretion, DOC loss, sinking, etc.) to accurately establish the carbon budget in these productive waters, where PP might be exported by other complex trophic pathways.

Conclusion

Our study investigated trophic interactions in the Gulf of Gabès to provide the first description of the PFW in the Southeastern Mediterranean area, where studies in marine food webs are still scarce. Despite the high productivity of the Gulf, different PFWs were observed, and the herbivorous food web was not observed during the spring diatom dominance, as is generally reported. The microzooplankton had the most important functional role in all the trophic pathways. The heterotrophic and mixotrophic protozoans, by having a broad prey size spectrum and various feeding behaviours, were able to remove substantial proportions of BP and PP from all size fractions and therefore participated actively in the carbon transfer. The shift of the PFW between seasons and stations was clearly related to the changes in the planktonic communities, whose spatial and seasonal dynamics are related to hydrodynamic and trophic features. The station influenced by the chemical loadings, even with low productivity, presented a PFW similar to those of the other stations with the same carbon transfer efficiency. This indicates that despite the potential chemical contamination, the trophic functioning was not modified, probably because of the buffer role of the hydrodynamics against pollutants. Further research is needed to assess the influence of chemical contamination coupled with the hydrodynamic features on the structure and functioning of planktonic food webs in these highly productive waters.

Supplementary Information The online version contains supplementary material available at https://doi.org/10.1007/s00027-023-00954-y.

Acknowledgements The study was carried out in the frame of the national projet GAMA (Gabès Modelling Assesment) funded by the National Institute for Marine Science and Technology (INSTM, Tunisia) and the project COZOMED-MERMEX (Effets of physical forcing on Coastal ZOoplankton community structure: study of the unusual case of a MEDiterranean ecosystem under strong tidal influence) funded by the French MAEE (ENVI-MED/MISTRALS AP 2014). English grammar and syntax of the manuscript were revised by Proof-Reading-Service.com. We thank two anonymous reviewers for their useful suggestions and comments.

Author contributions KMK: Conceptualization, Methodology, Investigation, Writing-original draft, Supervision. ABZ: Resources, Methodology, Investigations, Writing—review and editing. MM: Resources, Investigations. OC: Resources, Investigations. NN: Methodology, Investigation, Writing—review and editing. MT: Resources, Writing—review and editing. MP: Resources, Writing—review and editing. CS: Resources, Investigations. YK: Investigations, Software. MBH: Resources, Writing—review and editing. ASH: Project administration, Conceptualization, Methodology, Investigation, Writing—original draft, Supervision.

Data availability The datasets generated during and/or analyzed during the current study are available from the corresponding author on reasonable request.

Declarations

Conflict of interest There are no conflicts of interest for this study.

Ethical approval There are no ethical issues regarding this study.

References

Aberle N, Lengfellner K, Sommer U (2007) Spring bloom succession, grazing impact and herbivore selectivity of ciliate communities in response to winter warming. Œcologica 150:668–681

Alekseenko E, Raybaud V, Espinasse B, Carlotti F, Queguiner B, Thouvenin B, Garreau P, Baklouti M (2014) Seasonal dynamics and stoichiometry of the planktonic community in the NW Mediterranean Sea: a 3D modeling approach. Ocean Dyn 64:179–207

Almeda R, Calbet A, Alcaraz M, Saiz E, Trepat I, Arin L, Movilla J, Salo V (2011) Trophic role and carbon budget of metazoan microplankton in northwest Mediterranean coastal waters. Limnol Oceanogr 56:415–430

Alvain S, Moulin C, Dandonneau Y, Loisel H (2008) Seasonal distribution and succession of dominant phytoplankton groups in the global ocean: A satellite view. Global Biogeochemestry Cycles 22, GB3001, doi:https://doi.org/10.1029/2007GB003154

Aytan U, Feyzioglu AM, Valente A, Agirbas E, Fileman ES (2018) Microbial plankton communities in the coastal southeastern Black Sea: biomass, composition and trophic interactions. Oceanologia 60:139–152

Azam F, Fenchel T, Field JG, Gray JS, Meyer-Reil LA, Thingstad F (1983) The ecological role of water-column microbes in the sea. Mar Ecol Prog Ser 10:257–263

Bautista B, Harris RP (1992) Copepod gut contents, ingestion rates and grazing impact on phytoplankton in relation to size structure of zooplankton and phytoplankton during a spring bloom. Mar Ecol Prog Ser 82:41–50

Béjaoui B, Ben Ismail S, Othmani A, Hamida OBA-BH, Chevalier C, Feki-Sahnoun W, Harzallah A, Hamida NBH, Bouaziz R, Dahech S, Diaz F, Tounsi K, Sammari C, Pagano M, Bel Hassen M (2019) Synthesis review of the Gulf of Gabes (eastern Mediterranean Sea, Tunisia): morphological, climatic, physical, oceanographic, biogeochemical and fisheries features. Estuar Coas Shelf Sci 219:395–408

Bec B, Husseini-Ratrema J, Collos Y, Souchu P, Vaquer A (2005) Phytoplankton seasonal dynamics in a Mediterranean coastal lagoon: emphasis on the picoeukaryote community. J Plankton Res 27:881–894

Bel Hassen M, Drira Z, Hamza A, Ayadi H, Akrout F, Issaoui H (2008) Summer phytoplankton pigments and community composition related to water mass properties in the Gulf of Gabes. Estuar Coast Shelf Sci 77:645–656

Bel Hassen M, Drira Z, Hamza A, Ayadi H, Akrout F, Messaoudi S, Issaoui H, Aleya L, Bouaïn A (2009) Phytoplankton dynamics related to water mass properties in the Gulf of Gabès: ecological implications. J Marine Syst 75:216–226

Ben Brahim M, Hamza A, Hannachi I, Rebai A, Jarboui O, Bouain A, Aleya L (2010) Variability in the structure of epiphytic assemblages of Posidonia oceanica in relation to human interferences in the Gulf of Gabes, Tunisia. Mar Environ Res 70:411–421

Ben Lamine Y, Pringault O, Aissi M, Ensibi C, Mahmoudi E, Kefi ODY, Yahia MND (2015) Environmental controlling factors of copepod communities in the Gulf of Tunis (South western Mediterranean Sea). Cah Biol Mar 56:213–229

Ben Ltaief T, Drira Z, Devenon JL, Hamza A, Ayadia H, Pagano M (2017) How could thermal stratification affect horizontal distribution of depth-integrated metazooplankton communities in the Gulf of Gabes (Tunisia)? Mar Biol Res 13:269–287

Bérard-Therriault L, Poulin M, Bossé L (1999) Guide d'identification du phytoplancton marin de l'estuaire et du golfe du Saint-Laurent incluant également certains protozoaires. Publ. Spéc. Can, Sciences halieutique et aquatique, p 387p

Berggreen U, Hansen B, Kigkhoe AT (1988) Food size spectra, ingestion and growth of the copepod *Acartia tonsu* during development: Implications for determination of copepod production. Mar Biol 99:341–352

Berglund J, Müren U, Båmstedt U, Andersson A (2007) Efficiency of a phytoplankton-based and a bacteria-based food web in a pelagic marine system. Limnol Oceanogr 52:121–131

Bi R, Sommer U (2020) Food quantity and quality interactions at phytoplankton-zooplankton interface: chemical and reproductive responses in a calanoid copepod. Front Mar Sci 7:274

Boudaya L, Mosbahi N, Dauvin JC, Neifar L (2019) Structure of the benthic macrofauna of an anthropogenic influenced area: Skhira Bay (Gulf of Gabès, central Mediterranean Sea). Environ Sci Pollut Res 26:13522–13538

Boukthir M, Ben Jaberi, Chevalier C, Abdennadher J (2019) A high-resolution three dimensional hydrodynamic model of the Gulf of Gabes (Tunisia). 42nd 545 CIESM Congress

Boutrup PV, Moestrup Ø, Tillmann U, Daugbjerg N (2016) Katodinium glaucum (Dinophyceae) revisited: proposal of new genus, family and order based on ultrastructure and phylogeny. Phycologia 55(2):147–164

Brown SL, Landry MR, Christensen S, Garrison D, Gowing MM, Bidigare RR, Campbell L (2002) Microbial community dynamics and taxon-specific phytoplankton in the Arabian Sea. Deep Sea Research II 49:2345–2376

Buitenhuis ET, Rivkin RB, Sailley S, Le Quéré C (2010) Biogeochemical fluxes through microzooplankton. Glob Biogeochem 24:G4015

Calbet A (2008) The trophic roles of microzooplankton in marine systems. ICES J Mar Sci 65:325–331

Calbet A, Landry MR (2004) Phytoplankton growth, microzooplankton grazing, and carbon cycling in marine systems. Limnol Oceanogr 49:51–57

Calbet A, Saiz E (2005) The ciliate-copepod link in marine ecosystems. Aquat Microb Ecol 38:157–167

Calbet A, Alcaraz M, Saiz E, Estrada M, Trepat I (1996) Planktonic herbivorous food webs in the catalan Sea (NW Mediterranean): temporal variability and comparison of indices of phyto-zooplankton coupling based on state variables and rate processes. J Plankton Res 18:2329–2347

Calbet A, Martínez RA, Isari S, Zervoudaki S, Nejstgaard JC, Pitta P, Sazhin AF, Sousoni D, Gomes A, Berger SA, Tsagaraki TM, Ptacnik R (2012) Effects of light availability on mixotrophy and microzooplankton grazing in an oligotrophic plankton food web: evidences from a mesocosm study in Eastern Mediterranean waters. J Exp Mar Biol Ecol 424:66–77

Calbet A, Schmoker C, Russo F, Trottet A, Mahjoub MS, Larsen O, Tong HY, Drillet G (2016) Non-proportional bioaccumulation of trace metals and metalloids in the planktonic food web of two Singapore coastal marine inlets with contrasting water residence times. Sci Total Environ 560–561:284–294

Carstensen J, Klais R, Cloern JE (2015) Phytoplankton blooms in estuarine and coastal waters: Seasonal patterns and key species. Estuar Coast Shelf Sci 162:98–109

Chen M, Liu H, Chen B (2017) Seasonal variability of mesozooplankton feeding rates on phytoplankton in subtropical coastal and Estuarine Waters. Front Mar Sci 4:1–17

Chessel D, Mercier P (1993) Couplage de triplets statistiques et liaisons espèces-environnement. In: Lebreton JD, Asselain B (Eds). Biométrie et Environnement. Masson, Paris, pp 15-44

Chessel D, Hanafi M (1996) Analyses de la co-inertie de K nuages depoints. Rev Stat Appl 44:35–60

Christaki U, Van Wambeke F, Lefevre D, Lagaria A, Prieur L, Pujo-Pay M, Grattepanche JD (2011) Microbial food webs and metabolic state across oligotrophic waters of the Mediterranean Sea during summer. Biogeosciences 8:1839–1852

Courboulès J, Vidussi F, Soulié T, Mas S, Pecqueur D, Mostajir B (2021) Effects of experimental warming on small phytoplankton, bacteria and viruses in autumn in the Mediterranean coastal Thau Lagoon. Aquatic Ecol 55:647–666

Culhane CA, Perrière G, Considine EC, Cotter TG, Higgins DG (2002) Between group analysis of microarray data. Bioinformatics 18:1600–1608

Cushing DH (1989) A difference in structure between ecosystems in strongly stratified waters and in those that are only weakly stratified. J Plankton Res 11:1–13

d'Ortenzio F, d'Alcalà MR (2009) On the trophic regimes of the Mediterranean Sea: a satellite analysis. Biogeosciences 6(2):139–148

d'Alcalà MR, Conversano F, Corato F et al (2004) Seasonal pattern in plankton communities in a pluriannual time series at the coastal Mediterranean site (Gulf of Naples): an attempt to discern recurrences and trends. Sci Mar 68:65–83

Dagg MJ, Jackson GA, Checkley DM (2014) The distribution and vertical flux of faecal pellets from large zooplankton in Monterey bay and coastal California. Deep-Sea Res Part I-Oceanographic Res Papers 94:72–86

Dam HG, Peterson WT (1988) The effect of temperature on the gut clearance rate constant of planktonic copepods. J Exp Mar Biol Ecol 123:1–14

Davidson K, Gowen RJ, Tett P, Bresnan E, Harrison PJ, McKinney A, Milligan S, Mills DK, Silke J, Crooks AM (2012) Harmful algal blooms: how strong is the evidence that nutrient ratios and forms influence their occurrence? Estuar Coast Shelf Sci 115:399–413

Decembrini F, Caroppo C, Azzaro M (2009) Size structure and production of phytoplankton community and carbon pathways channeling in the Southern Tyrrhenian Sea (Western Mediterranean). Deep Sea Res Part II 56:687–699

Decembrini F, Caroppo C, Caruso G, Bergamasco A (2021) Linking microbial functioning and trophic pathways to ecological status in a coastal mediterranean ecosystem. Water 13:1325

Deng XW, Chen J, Hansson LA, Zhao X, Xie P (2020) Eco-chemical mechanisms govern phytoplankton emissions of dimethylsulfide in global surface waters. Nat Sci Rev. https://doi.org/10.1093/nsr/nwaa140

Dokulil MT, Qian K (2021) Photosynthesis, carbon acquisition and primary productivity of phytoplankton: a review dedicated to Colin Reynolds. Hydrobiologia 848:77–94. https://doi.org/10.1007/s10750-020-04321-y

Dolédec S, Chessel D (1987) Rythmes saisonniers et composantes stationnelles en milieu aquatique. I- Description d'un plan d'observations complet par projection de variables. Acta Œcologica, Œcologica Generalis 8:403–426

Dolédec S, Chessel D (1989) Rythmes saisonniers et composantes stationnelles en milieu aquatique II—Prise en compte et élimination d'effets dans un tableau faunistique. Acta Œcologica, Œcologica Generalis 10:207–232

Dolédec S, Chessel D (1994) Co-inertia analysis: an alternative method for studying species environment relationships. Freshw Biol 31:277–294

Drira Z, Bel Hassen M, Hamza A, Rebai A, Bouain A, Ayadi H, Aleya L (2009) Spatial and temporal variations of microphytoplankton composition related to hydrographic conditions in the Gulf of Gabes. J Mar Biol Assoc UK 89:1559–1569

Drira Z, Bel Hassen M, Ayadi H, Aleya L (2014) What factors drive copepod community dynamics in the Gulf of Gabes, Eastern Mediterranean Sea? Environ Sci Pollut Res 21:2918–2934

Drira Z, Sahnoun H, Ayadi H (2017) Spatial distribution and source identification of heavy metals in surface waters of three coastal areas of Tunisia. Development 5:27

Drira Z, Hamza A, Bel Hassen M, Ayadi H, Bouaïn A, Aleya L (2008) Dynamics of dinoflagellates and environmental factors during the summer in the Gulf of Gabes (Tunisia, Eastern Mediterranean Sea). Sci Mar 72:59–71

Duarte CM, Agustí S, Vaque D, Agawin NSR, Felipe J, Casamayor EO, Gasol JM (2005) Experimental test of bacteria-phytoplankton coupling in the Southern Ocean. Limnol Oceanogr 50:1844–1854

El Kateb A, Stalder C, Rüggeberg A, Neururer C, Spangenberg JE, Spezzaferri S (2018) Impact of industrial phosphate waste discharge on the marine environment in the Gulf of Gabes (Tunisia). PLoS One 13(5):e0197731

Feng C, Han MQ, Dong CC, Jia JY, Chen JW, Wong CK (2020) Mesozooplankton selective feeding on phytoplankton in a semi-enclosed bay as revealed by HPLC pigment analysis. Water 12:2031

Feki-Sahnoun W, Hamza A, Mahfoudi M, Rebai A, Bel Hassen M (2014) Long-term microphytoplankton variability patterns using multivariate analyses: ecological and management implications. Environ Sci Pollut Res 21:11481–11499

Feki-Sahnoun W, Hamza A, Njah H, Barraj N, Mahfoudi M, Rebai A, Bel Hassen M (2017) Bayesian network approach to determine environmental factors controlling Karenia selliformis occurrences and blooms in the Gulf of Gabès, Tunisia. Harmful Algae 63:119–132

Feki-Sahnoun W, Njah H, Hamza A, Barraj N, Mahfoudi M, Rebai A, Bel Hassen M (2018) Using general linear model, Bayesian networks and naive Bayes classifier for prediction of *Karenia selliformis* occurrences and blooms. Eco Inform 43:12–23

Feki-Sahnoun W, Njah H, Hamza A, Barraj N, Mahfoudi M, Rebai A, Bel Hassen M (2020) Using a naive Bayes classifier to explore the factors driving the harmful dinoflagellate Karenia selliformis blooms in a Southeastern Mediterranean lagoon. Ocean Dyn 70:897–911

Fonda Umani S, Beran A (2003) Seasonal variations in the dynamics of microbial plankton communities: first estimates from experiments in the Gulf of Trieste, Northern Adriatic Sea. Mar Ecol Prog Ser 247:1–16

Fonda Umani S, Tirelli V, Beran A, Guardiana B (2005) Relationships between microzooplankton and mesozooplankton: competition versus predation on natural assemblages of the Gulf of Trieste (northern Adriatic Sea). J Plankton Res 27:973–986

Gallegos CL (1989) Microzooplankton grazing on phytoplankton in the Rhode River, Maryland: non-linear feeding kinetics. Mar Ecol Prog Ser 57:22–33

Gentleman W, Leising A, Frost B, Strom S, Murray J (2003) Functional responses for zooplankton feeding on multiple resources: a review of assumptions and biological dynamics. Deep Sea Res Part II 50:2847–2875

Giannakourou A, Tsiola A, Kanellopoulou M, Magiopoulos I, Siokou F, Pitta P (2014) Temporal variability of the microbial food web (viruses to ciliates) under the influence of the Black Sea Water inflow (N. Aegean, E. Mediterranean). Mediterr Mar Sci 15:769–780

Girault M, Arakawa H, Hashihama F (2013) Phosphorus stress of microphytoplankton community in the western subtropical North Pacific. J Plankton Res 35:146–157

Gómez F, Claustre H, Raimbault P, Souissi S (2007) Two high-nutrient low-chlorophyll phytoplankton assemblages: the tropical central Pacific and the offshore Perú-Chile Current. Biogeosciences 41:101–1113

Grami B, Niquil N, Sakka Hlaili A, Gosselin M, Hamel D, Hadj Mabrouk H (2008) The plankton food web of the Bizerte Lagoon (South-Western Mediterranean): II. Carbon steady state modelling using inverse analysis. Estuar Coast Shelf Sci 79:101–113

Grattepanche JD, Vincent D, Breton E, Christaki U (2011) Microzooplankton herbivory during the diatom Phaeocystis spring succession in the eastern English Channel. J Exp Mar Biol Ecol 404:87–97

Greve W, Reiners F, Nast J, Hoffmann S (2004) Helgoland roads meso- and macrozooplankton time-series 1974 to 2004: lessons from 30 years of single spot, high frequency sampling at the only offshore island of the North Sea. Helgol Mar Res 58:274–288

Grinienė E, Šulčius S, Kuosa H (2016) Size-selective microzooplankton grazing on the phytoplankton in the Curonian Lagoon (SE Baltic Sea). Oceanologia 58:292–301

Hamdi I, Denis M, Bellaaj-Zouari A, Khemakhem H, Bel Hassen M, Barani A, Bezac C, Maalej S (2015) The characterization and summer distribution of ultraphytoplankton in the Gulf of Gabès (Eastern Mediterranean Sea, Tunisia) by using flow cytometry. Cont Shelf Res 93:27–38

Hamza IS, Feki-Sahnoun W, Hamza A, Bel Hassen M (2016) Long term characterization of *Trichodesmium erythraeum* blooms in Gabès Gulf (Tunisia). Cont Shelf Res 124:95–103

Hannachi I, Drira Z, Bel Hassen M, Hamza A, Ayadi H, Bouain A, Aleya L (2008) Abundance and biomass of the ciliate community during a spring cruise in the gulf of Gabes (East Mediterranean Sea, Tunisia). Acta Protozoologica 47:293–305

Hannides CCS, Siokou I, Zervoudaki S, Frangoulis C, Lange MA (2015) Mesozooplankton biomass and abundance in Cyprus coastal waters and comparison with the Aegean Sea (Eastern Mediterranean). Mediterr Mar Sci 16:373–384

Hargraves PE (2002) The ebridian flagellates *Ebria* and *Hermesinum*. Plankton Biol Ecol 49:9–16

Irigoien X (1998) Gut clearance rate constant, temperature and initial gut contents: a review. J Plankton Res 20(5):997–1003

Jacobson DM, Anderson DM (1996) Widespread phagocytosis of ciliates and other protists by marine mixotrophic and heterotrophic thecate dinoflagellates. J Phycol 32:279–285

Jafari F, Ramezanpour Z, Sattari M (2015) First record of *Ebria tripartita* (Schumann) Lemmermann, 1899 from south of the Caspian Sea. Caspian J Environ Sci 13(3):283–288

Jeong HJ, Yoo YD, Kim ST, Kang NS (2004) Feeding by the heterotrophic dinoflagellate *Protoperidinium bipes* on the diatom *Skeletonema costatum*. Aquatic Microbiol Ecol 36:171–179

Jeong HJ, Yoo YD, Park JY, Song JY, Kim ST, Lee SH, Kim KY, Yih WH (2005) Feeding by the phototrophic red-tide dinoflagellates: five species newly revealed and six species previously known to be mixotrophic. Aquat Microb Ecol 40:133–155

Jeong HJ, Yoo YD, Kim JS, Seong KA, Kang NS, Kim TH (2010) Growth, feeding and ecological roles of the mixotrophic and heterotrophic dinoflagellates in marine planktonic food webs. Ocean Sci J 45:65–91

Kase L, Metfes K, Kraberg AC, Neuhaus S, Meunier CL, Wiltshire KH, Boersma M (2021) Metabarcoding analysis suggests that fexible food web interactions in the eukaryotic plankton community are more common than specific predator–prey relationships at Helgoland Roads, North Sea. ICES J Mar Sci 78:3372–3386

Khammeri Y, Hamza IS, Bellaaj Zouari A, Hamza A, Sahlia E, Akrout F, Ben Kacem MY, Messaoudi S, Bel Hassen M (2018) Atmospheric bulk deposition of dissolved nitrogen, phosphorus and silicate in the Gulf of Gabès (South Ionian Basin); implications for marine heterotrophic prokaryotes and ultraphytoplankton. Cont Shelf Res 159:1–11

Khammeri Y, Bellaaj-Zouari A, Hamza A, Medhioub W, Sahli E, Akrout F, Barraj N, Ben Kacem MY, Bel Hassen M (2020) Ultraphytoplankton community composition in Southwestern and Eastern Mediterranean Basin: relationships to water mass properties and nutrients. J Sea Res 158:101875. https://doi.org/10.1016/j.seares.2020.101875

Khedhri I, Djabou H, Afli A (2014) Trophic and functional organization of the benthic macrofauna in the lagoon of Boughrara–Tunisia (SW Mediterranean Sea). J Mar Biological Assoc UK 95:647–659

Kleppel G, Pieper R (1984) Phytoplankton pigments in the gut contents of planktonic copepods from coastal waters off Southern California. Mar Biol 78:193–198. https://doi.org/10.1007/BF00394700

Kmiha Megdiche S, Drira Z, Pagano M, Ayadi H (2019) Changes in copepod community between two contrasting samplings in a highly polluted Mediterranean coastal zone (Sfax Bay, Tunisia). Oceanogr Fish Open Access J. https://doi.org/10.19080/OFOAJ.2019.10.555785

Landry MR, Calbet A (2004) Microzooplankton production in the oceans. ICES J Mar Sci 61:501–507

Landry MR, Décima MR (2017) Protistan microzooplankton and the trophic position of tuna: quantifying the trophic link between micro- and mesozooplankton in marine foodwebs. ICES J Mar Sci 74:1885–1892

Landry MR, Hassett RP (1982) Estimating the grazing impact of marine Micro-zooplankton. Mar Biol 67:283–288

Landry MR, Brown SL, Neveux J, Dupouy C, Blanchot J, Christensen S, Bidigare RR (2003) Phytoplankton growth and microzooplankton grazing in high-nutrient, low chlorophyll waters of the equatorial Pacific: community and taxon-specific rate assessments from pigment and flow cytometric analyses. J Geophys Res 108:8142

Lê S, Josse J, Husson F (2008) FactoMineR: an R package for multivariate analysis. J Stat Softw 25:1–18

Leblanc K, Queguiner B, Diaz F, Cornet V, Michel-Rodriguez M, De Madron XD, Bowler C, Malviya S, Thyssen M, Grégori G, Rembauville M, Grosso O, Poulain J, De Vargas C, Pujo-Pay M, Conan P (2018) Nanoplanktonic diatoms are globally overlooked but play a role in spring blooms and carbon export. Nat Commun 9(1):953

Legendre L, Gosselin M (1989) New production and export of organic matter to the deep ocean: consequences of sorne recent discoveries. Limnol Oceanogr 34:1374–1380

Legendre L, Le Fèvre J (1989) Hydrodynamical singularities as controls of recycled versus export production in oceans. In: Berger WH, Smetacek VS, Wefer G (eds) Productivity of the ocean: present and past. John Wiley and sons Limited, Dahlem, pp 49–63

Legendre L, Rassoulzadegan F (1995) Plankton and nutrient dynamics in marine waters. Ophelia 41:153–172

Liu X, Li Y, Wu Y, Huang B, Dai M, Fu F, Hutchins DA, Gao K (2017) Effects of elevated CO_2 on phytoplankton during a mesocosm experiment in the southern eutrophicated coastal water of China. Sci Rep 7:6868

Livanou E, Lagaria A, Santi I, Mandalakis M, Pavlidou A, Lika K, Psarra S (2019) Pigmented and heterotrophic nanoflagellates: abundance and grazing on prokaryotic picoplankton in the ultra-oligotrophic Eastern Mediterranean Sea. Deep Sea Res Part II 164:100–111

López-Abbate MC (2021) Microzooplankton communities in a changing ocean: a risk assessment. Diversity 13:82

Makhlouf Belkahia N, Pagano M, Chevalier C, Devenon JL, Daly Yahia MN (2021) Zooplankton abundance and community structure driven by tidal currents in a Mediterranean coastal lagoon (Boughrara, Tunisia, SW Mediterranean Sea). Estuar Coast Shelf Sci 250:107101

Marrec P, Heather MN, Gayantonia F, Françoise M, Jacob PS, Menden-Deuer S (2021) Seasonal variability in planktonic food web structure and function of the Northeast U.S. Shelf. Limnol Oceanogr 66:1440–1458. https://doi.org/10.1002/lno.11696

Meddeb M, Grami B, Chaalali A, Haraldsson H, Niquil N, Pringault O, Sakka Hlaili A (2018) Plankton food-web functioning in anthropogenically impacted coastal waters (SW Mediterranean Sea): an ecological network analysis. Prog Oceanogr 162:66–82

Meddeb M, Niquil N, Grami B, Mejri K, Haraldsson M, Chaalali A, Pringault O, Sakka Hlaili A (2019) A new type of plankton food web functioning in coastal waters revealed by coupling Monte Carlo Markov chain linear inverse method and ecological network analysis. Ecol Ind 104:67–85

Mercado JM, Cortés D, Gómez-Jakobsen F, García-Gómez C, Ouaissa S, Yebra L, Ruíz JM (2021) Role of small-sized phytoplankton in triggering an ecosystem disruptive algal bloom in a Mediterranean hypersaline coastal lagoon. Mar Pollut Bull 164:111989

Moigis AG, Gocke K (2003) Primary production of phytoplankton estimated by means of the method in coastal waters. J Plankton Res 25:1291–1300

Morales CE, Harris RP, Head RN, Tranter PRG (1993) Copepod grazing in the oceanic northeast Atlantic during a 6 week drifting station: the contribution of size classes and vertical migrants. J Plankton Res 15:185–211

Morán XAG, Ducklow HW, Erickson M (2011) Single-cell physiological structure and growth rates of heterotrophic bacteria in a temperate estuary (Waquoit Bay, Massachusetts). Limnol Oceanogr 56:37–48

Ning X, Li W, Cai YM, Shi J (2005) Comparative analysis of bacterioplankton and phytoplankton in three ecological provinces of the northern South China Sea. Mar Ecol Prog Ser 293:17–28

Numerical and Taxonomic Index of ICES Plankton Identification Leaflets, 1939–2001

Othmani A, Béjaoui B, Chevalier C, Elhmaidi D, Devenon JL, Aleya L (2017) High-resolution numerical modelling of the barotropic tides in the Gulf of Gabes, eastern Mediterranean Sea (Tunisia). J Afr Earth Sc 129:224–232

Paklar GB, Vilibić I, Grbec B, Matić F, Mihanović H, Džoić T, Šantić D, Šestanović S, Šolić M, Ivatek-Šahdan S, Kušpilić G (2020) Record-breaking salinities in the middle Adriatic during summer 2017 and concurrent changes in the microbial food web. Prog Oceanogr 185:102345

Parsons TP, Maita Y, Lalli CM (1984) A manuel of chemical and biological methods for seawater analysis. Pergamon Press, Oxford, England 1:173

Pecqueur D, Vidussi F, Fouilland E, Le Floc'h E, Mas S, Roques C, Salles C, Tournoud MG, Mostajir B (2011) Dynamics of microbial planktonic food web components during a river flash flood in a Mediterranean coastal lagoon. Hydrobiologia 673:13–27

Pecqueur D, Courboulès J, Roques C, Mas S, Pete R, Vidussi F, Mostajir B (2022) Simultaneous study of the growth and grazing mortality rates of microbial food web components in a Mediterranean Coastal Lagoon. Diversity 14(3):186

Pulido-Villena E, Baudoux AC, Obernosterer I, Landa M, Caparros J, Catala P, Georges C, Harmand J, Guieu C (2014) Microbial food web dynamics in response to a Saharan dust event: results from a mesocosm study in the oligotrophic Mediterranean Sea. Biogeosci Discuss 11:337–371

Quemeneur M, Bel Hassen M, Armougom F, Khammeri Y, Lajnef R (2020) Prokaryotic diversity and distribution along physical and nutrient gradients in the tunisian Coastal Waters (South Mediterranean Sea). Front Microbiol 11:593540

Raimbault P, Garcia N, Cerutti F (2008) Distribution of inorganic and organic nutrients in the South Pacific Ocean−evidence for long-term accumulation of organic matter in nitrogen-depleted waters. Biogeosciences 5(2):281–298

Rhyter JH (1969) Photosynthesis and fish production in the sea. Science 166:72–76

Romano F, Symiakaki K, Pitta P (2021) Temporal variability of planktonic ciliates in a coastal oligotrophic environment: mixotrophy, size classes and vertical distribution. Front Mar Sci 8:113p

Ross ON, Fraysse M, Pinazo C, Pairaud I (2016) Impact of an intrusion by the Northern Current on the biogeochemistry in the eastern Gulf of Lion, NW Mediterranean. Estuar Coast Shelf Sci 170:1–9

Saito H, Ota T, Suzuki K, Nishioka J, Tsuda A (2006) Role of heterotrophic dinoflagellate *Gyrodinium* sp. in the fate of an iron induced diatom bloom. Geophys Res Lett 33:L09602

Saiz E, Rodriguez V, Alcaraz M (1992) Spatial distribution and feeding rates of *Centropages typicus* in relation to frontal hydrographic structures in the Catalan Sea (Western Mediterranean). Mar Biol 112:49–56

Sakka Hlaili A, Grami B, Hadj Mabrouk H, Gosselin M, Hamel D (2007) Phytoplankton growth and microzooplankton grazing rates in a restricted Mediterranean lagoon (Bizerte Lagoon, Tunisia). Mar Biol 151:767–783

Sakka Hlaili A, Grami B, Niquil N, Gosselin M, Hamel D, Troussillier M (2008) The planktonic food web of the Bizerte lagoon (South-Western Mediterranean) during summer: I. Spatial distribution under different anthropogenic pressures. Estuar Coast Shelf Sci 78:61–77

Sakka Hlaili A, Niquil N, Legendre L (2014) Planktonic food webs revisited Reanalysis of results from the linear inverse approach. Prog Oceanogr 120:216–229

Salgado-Hernanz PM, Racault MF, Font-Muñoz JS, Basterretxea G (2019) Trends in phytoplankton phenology in the Mediterranean Sea based on ocean-colour remote sensing. Remote Sens Environ 221:50–64

Sammari C, Koutitonsky VG, Moussa M (2006) Sea level variability and tidal resonance in the Gulf of Gabes. Tunisia. Cont Shelf Res 26(3):338–350

Sandhu SK, Morozov AY, Mitra A, Flynn K (2019) Exploring nonlinear functional responses of zooplankton grazers in dilution experiments via optimization techniques. Limnol Oceanogr 64:774–784

Šantić D, Krstulović N, Šolić M, Kušpilić G (2011) Distribution of *Synechococcus* and *Prochlorococcus* in the central Adriatic Sea. Acta Adriat 52:101–114

Sato M, Yoshikawa T, Takeda S, Furuya S (2007) Application of the size-fractionation method to simultaneous estimation of clearance rates by heterotrophic flagellates and ciliates of pico- and nanophytoplankton. J Exp Mar Biol Ecol 349:334–343

Sautour B, Artigas LF, Delmas D, Herbland A, Laborde P (2000) Grazing impact of micro-and mesozooplankton during a spring situation in coastal waters off the Gironde estuary. J Plankton Res 22(3):531–552

Seong KA, Jeong HJ, Kim S, Kim GH, Kang JH (2006) Bacterivory by co-occurring red-tide algae, heterotrophic nanoflagellates, and ciliates on marine bacteria. Mar Ecol Prog Ser 322:85–97

Sherr EB, Sherr BF (1993) Preservation and storage of samples for enumeration of heterotrophic protests. In: Kemp PF, Sherr BF, Sherr EB, Cole JJ (eds) Handbook of methods in aquatic microbial ecology. Lewis Publishers, London, pp 207–212

Sherr EB, Sherr BF, Hartz AJ (2009) Microzooplankton grazing impact in the western Arctic Ocean. Deep-Sea Res II. https://doi.org/10.1016/jdsr2.2008.10.036

Shinada A, Ban S, Yamada Y, Ikeda T (2005) Seasonal variations of plankton food web structure in the coastal water off Usujiri southwestern Hokkaido, Japan. J Oceanogr 61:645–654

Šimek K, Bobkova J, Macek M, Nedoma J, Psenner R (1995) Ciliate grazing on picoplankton in a eutrophic reservoir during the summer phytoplankton maximum: A study at the species and community level. Limnol Oceanogr 40:1077–1090

Siokou-Frangou I, Christaki U, Mazzocchi MG, Montresor M, d'Alcala MR, Vaque D, Zingone A (2010) Plankton in the open Mediterranean Sea: a review. Biogeosciences 7(5):1543–1586

Slaughter AM, Bollens SM, Bollens GR (2006) Grazing impact of mesozooplankton in an upwelling region off northern California, 2000–2003. Deep Sea Res II 53:3099–3115

Šolić M, Krstulović N, Kušpilić G, Ninčević Gladan Ž, Bojanić N, Šestanović S, Šantić D, Ordulj M (2010) Changes in microbial food web structure in response to changed environmental trophic status: a case study of the Vranjic Basin (Adriatic Sea). Mar Environ Res 70:239–249

Stoecker DK (1999) Mixotrophy among dinoflagellates. J Eukaryot Microbiol 46:397–401

Sun J, Feng Y, Zhang Y, Hutchins DA (2007) Fast microzooplankton grazing on fast growing, low-biomass phytoplankton: a case study in spring in Chesapeake Bay, Delaware Inland Bays and Delaware Bay. Hydrobiologia 589(1):127–139

Tanaka T, Rassoulzadegan F, Thingstad TF (2003) Measurements of phosphate affinity constants and phosphorus release rates from the microbial food web in Villefranche Bay, northwestern Mediterranean. Limnol Oceanogr 48:1150–1160

Tanaka T, Thingstad TF, Christaki U, Colombet J, CornetBarthaux V, Courties C, Grattepanche JD, Lagaria A, Nedoma J, Oriol L, Psarra S, Pujo-Pay M, Van Wambeke F (2011) Lack of P-limitation of phytoplankton and heterotrophic prokaryotes in surface waters of three anticyclonic eddies in the stratified Mediterranean Sea. Biogeosciences 8:525–538

Thompson RM, Brose U, Sunne JA, Hall RO, Hladyz S, Kitching RL, Martinez ND, Rantala H, Romanuk TN, Stouffer DB, Tylianakis JM (2012) Food webs: reconciling the structure and function of biodiversity. Trends Ecol Evol 27:689–697

Trégouboff G, Rose M (1957) Manuel de Planctonologie Méditerranéenne. Centre National de la Recherche Scientifique, Paris 1:587

Tseng LC, Kumar R, Dahms HU, Chen QC, Hwang JS (2008) Copepod gut contents, ingestion rates and feeding impact in relation to their size structure in the southeastern Taiwan Strait. Zoological Studies 47(4):402–416

Utermöhl H (1931) Neue Wege in der quantitativen Erfassung des Plankton. (Mit besonderer Berücksichtigung des Ultraplanktons). Vereinigung Für Theoretische und Angewandte Limnologie 5:567–596

Vargas CA, Martínez RA, Cuevas LA, Pavez MA, Cartes C, Humberto E, González HE, Escribano R, Daneri G (2007) The relative importance of microbial and classical food webs in a highly productive coastal upwelling area. Limnol Oceanogr 52(4):1495–1510

Vézina AF, Pahlow M (2003) Reconstruction of ecosystem flows using inverse methods: how well do they work? J Mar Syst 40:55–77

Viñas MD, Negri RM, Cepeda GD, Hernández D, Silva R, Daponte MC, Capitanio FL (2013) Seasonal succession of zooplankton in coastal waters of the Argentine Sea (Southwest Atlantic Ocean): prevalence of classical or microbial food webs. Mar Biol Res 9:371–382

Zakaria HY, Hassan AKM, El-Naggar HA, Abo-Senna FM (2018) Biomass determination based on the individual volume of the dominant copepod species in the Western Egyptian Mediterranean Coast. Egypt J Aquatic Res 44:89–99

Zmemla R, Chaurand P, Benjdidia M, Elleuch B, Bottero JY (2016) Characterization and pH dependent leaching behavior of tunisian phosphogypsum. Am Sci Res J Eng, Technol Sci (ASRJETS) 24:230–244